NASA/TP–2016-219194

Radio Frequency Plasma Synthesis of Boron Nitride Nanotubes (BNNTs) for Structural Applications: Part II

Stephen J. Hales
Langley Research Center, Hampton, Virginia

Joel A. Alexa
Analytical Mechanics Associates, Inc., Hampton, Virginia

Brian J. Jensen
Langley Research Center, Hampton, Virginia

May 2016

NASA STI Program . . . in Profile

Since its founding, NASA has been dedicated to the advancement of aeronautics and space science. The NASA scientific and technical information (STI) program plays a key part in helping NASA maintain this important role.

The NASA STI program operates under the auspices of the Agency Chief Information Officer. It collects, organizes, provides for archiving, and disseminates NASA's STI. The NASA STI program provides access to the NTRS Registered and its public interface, the NASA Technical Reports Server, thus providing one of the largest collections of aeronautical and space science STI in the world. Results are published in both non-NASA channels and by NASA in the NASA STI Report Series, which includes the following report types:

- TECHNICAL PUBLICATION. Reports of completed research or a major significant phase of research that present the results of NASA Programs and include extensive data or theoretical analysis. Includes compilations of significant scientific and technical data and information deemed to be of continuing reference value. NASA counter-part of peer-reviewed formal professional papers but has less stringent limitations on manuscript length and extent of graphic presentations.

- TECHNICAL MEMORANDUM. Scientific and technical findings that are preliminary or of specialized interest, e.g., quick release reports, working papers, and bibliographies that contain minimal annotation. Does not contain extensive analysis.

- CONTRACTOR REPORT. Scientific and technical findings by NASA-sponsored contractors and grantees.

- CONFERENCE PUBLICATION. Collected papers from scientific and technical conferences, symposia, seminars, or other meetings sponsored or co-sponsored by NASA.

- SPECIAL PUBLICATION. Scientific, technical, or historical information from NASA programs, projects, and missions, often concerned with subjects having substantial public interest.

- TECHNICAL TRANSLATION. English-language translations of foreign scientific and technical material pertinent to NASA's mission.

Specialized services also include organizing and publishing research results, distributing specialized research announcements and feeds, providing information desk and personal search support, and enabling data exchange services.

For more information about the NASA STI program, see the following:

- Access the NASA STI program home page at http://www.sti.nasa.gov

- E-mail your question to help@sti.nasa.gov

- Phone the NASA STI Information Desk at 757-864-9658

- Write to:
  NASA STI Information Desk
  Mail Stop 148
  NASA Langley Research Center
  Hampton, VA 23681-2199

NASA/TP–2016-219194

Radio Frequency Plasma Synthesis of Boron Nitride Nanotubes (BNNTs) for Structural Applications: Part II

Stephen J. Hales
Langley Research Center, Hampton, Virginia

Joel A. Alexa
Analytical Mechanics Associates, Inc., Hampton, Virginia

Brian J. Jensen
Langley Research Center, Hampton, Virginia

National Aeronautics and
Space Administration

Langley Research Center
Hampton, Virginia 23681-2199

May 2016

Available from:

NASA STI Program / Mail Stop 148
NASA Langley Research Center
Hampton, VA 23681-2199
Fax: 757-864-6500

Abstract

Boron nitride nanotubes (BNNTs) are more thermally and chemically compatible with metal- and ceramic-matrix composites than carbon nanotubes (CNTs). The lack of an abundant supply of defect-free, high-aspect-ratio BNNTs has hindered development as reinforcing agents in structural materials. Recent activities at the National Research Council – Canada (NRC-C) and the University of California – Berkeley (UC-B) have resulted in bulk synthesis of few-walled, small diameter BNNTs. Both processes employ induction plasma technology to create boron vapor and highly reactive nitrogen species at temperatures in excess of 8000 K. Subsequent recombination under controlled cooling conditions results in the formation of BNNTs at a rate of 20 g/hr and 35 g/hr, respectively. The end product tends to consist of tangled masses of fibril-, sheet-, and cotton candy-like materials, which accumulate within the processing equipment.

The radio frequency plasma spray (RFPS) facility at NASA Langley Research Center (LaRC), developed for metallic materials deposition, has been re-tooled for in-situ synthesis of BNNTs. The NRC-C and UC-B facilities comprise a 60 kW RF torch, a reactor with a stove pipe geometry, and a filtration system. In contrast, the LaRC facility has a 100 kW torch mounted atop an expansive reaction chamber coupled with a cyclone separator. The intent is to take advantage of both the extra power and the equipment configuration to simultaneously produce and gather BNNTs in a macroscopic form amenable to structural material applications. Reverse engineering of the incumbent methods permits the processing parameters to be used as a guideline for the LaRC effort. The ultimate objectives include (a), the generation of a predominantly “cotton candy”-like product, and (b), in-line sorting of the crude product using dry separation techniques.

Table of Contents

Table of Figures

Table of Tables

Symbols and Abbreviations

Abbreviations

Ar .....argon

B .....boron

BN .....boron nitride

BNNT.....boron nitride nanotube

CNT.....carbon nanotube

DC .....direct current

EPIC.....extended-pressure, inductively-coupled

H_2 .....hydrogen

HABS .....hydrogen-assisted BNNT synthesis

h-BN.....hexagonal boron nitride

He.....helium

ICP .....inductively-coupled plasma

K.....Kelvin

LaRC .....Langley Research Center

LPS###.....Langley Plasma Spray Number

N_2 .....nitrogen

NRC-C .....National Research Council – Canada

NT .....nanotube

PF .....powder feeder

RF.....radio frequency

RFPS .....radio frequency plasma spray

rpm .....revolutions per minute

slpm.....standard liters per minute

SWNT .....single-walled nanotube

T .....temperature

TGA .....thermo-gravimetric analysis

UC-B .....University of California – Berkeley

1. Introduction

1.1. Background

The impetus for this report stems from the potential increase in performance to be gained by employing nanotubes (NTs) in multi-functional aerospace structures. The room temperature, specific tensile properties of defect-free, single-walled nanotubes (SWNT) and candidate materials for vehicle structures are presented in figure 1 [ref. 1]. The density-compensated modulus and strength of NTs and materials containing NTs are compared with select fiber reinforcing agents and metal-, polymer-, or carbon-matrix composites. On a theoretical basis, the potential increase in tensile properties offered by SWNTs is an order of magnitude. Such a breakthrough improvement would expand engineering design space, but realistically these values may only be considered as a target. As with all engineering materials, the presence of defects will undoubtedly render this limit unattainable. Specific modulus and strength values reported in the literature also vary widely as a result of the cross-sectional area selected to calculate density and stress. Experimental results from reliable sources for materials containing carbon nanotubes (CNTs) and boron nitride nanotubes (BNNTs) are included in figure 1 [refs. 2–5]. Noting the log scale, the NT-related data reveal a significant strength improvement over state-of-the-art fiber reinforcements and advanced composites.

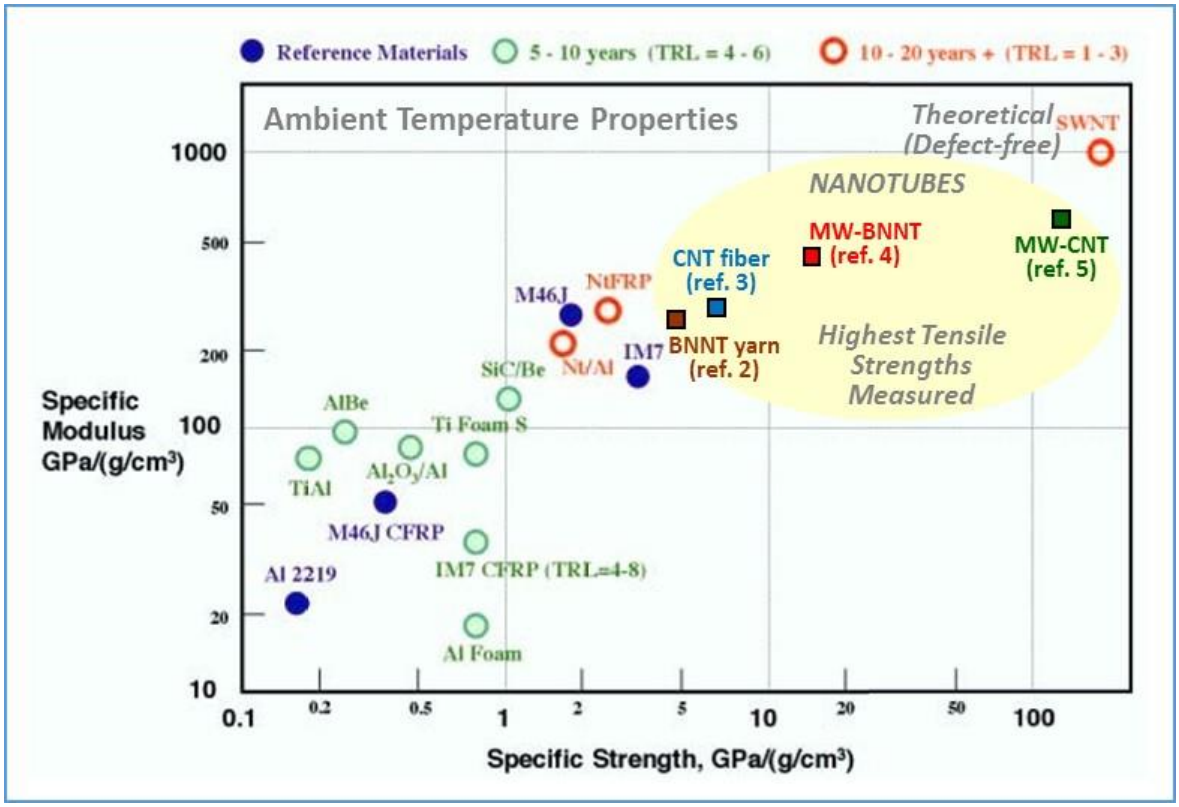

Figure 1. The density-compensated modulus and strength of nanotube-containing materials are compared with incumbent reinforcing agents and composites [ref. 1]. The theoretical properties of SWNTs, and some verifiable measured properties for CNT- and BNNT-based materials are included [refs. 2–5].

BNNTs are a structural analog of CNTs, i.e., the carbon atoms are alternately replaced by boron and nitrogen atoms. Similar to CNTs, high-purity, low-defect BNNTs exhibit extremely high strength and stiffness but possess better chemical and thermal stability than CNTs [ref. 6]. This results in a broader range of structural applications, particularly as reinforcing agents for metal- and ceramic-matrix composites or hybrid laminates. In contrast with CNTs, BNNTs are dielectrics and exhibit a high neutron absorption cross-section [ref. 7]. First, the low conductivity of BNNTs negates the galvanic imbalance which would be created at reinforcement interfaces in CNT-containing metal matrix composites. Second, the potential exists to create multi-functional structures, such as for radiation protection [ref. 8]. For most applications, the quality of NTs can be equated with microscopic characteristics, i.e., crystallinity, purity, and number of walls [ref. 6]. These requirements can be extended for composite material usage to include macroscopic characteristics, such as NT length, diameter, and aspect ratio.

The race to mass produce high quality BNNTs has been ongoing since they were first synthesized in 1995 [ref. 9]. The lack of a reliable and reproducible method for mass production of such high quality BNNTs has hindered the development of applications in fiber form, or as matrix reinforcing agents. Small quantities of varying quality have yielded encouraging results, but it is apparent from the data included in figure 1 that there is much room for improvement. The combined results of world-wide research activities suggest that the physical characteristics of BNNTs are strongly dependent on the production method employed. Among methods investigated, high temperature processes seem best poised to achieve the elusive goal.

Although it has been the front-runner in terms of quality for many years, the laser-vaporization method pioneered by Smith et al. still suffers from low throughput (~100 mg/h) and is confined to batch processing [ref. 10]. Inductively-coupled plasma (ICP) synthesis technology has emerged as the most viable candidate. In contrast with high velocity / low volume, direct current (DC) plasmas, the low velocity / high volume characteristics of ICP techniques offer extended dwell times in the reaction zone. The velocity is lowered from 600–2300 ms^{-1} to 300–400 ms^{-1}, and the internal diameter of the torch is raised from 6–8 mm to 35–70 mm [ref. 11]. Longer residence times and larger plasma plumes are much more effective at processing mass quantities. As a consequence, the research at two institutions is close to fruition and is summarized below.

1.1.1. University of California – Berkeley (UC-B)

The BNNT synthesis facility developed at UC-B is referred to as the extended-pressure, inductively-coupled (EPIC) plasma system shown in figure 2 [ref. 12]. The approach represents a natural extension of an earlier campaign to produce BNNTs via DC plasma synthesis techniques [ref. 13]. The facility consists of a 60 kW Tekna RF torch mounted on top of a "stove-pipe" reaction/quenching chamber coupled with filtration devices and an exhaust system. The internal dimensions of the ceramic-lined reactor are ~1.2 m long by ~0.15 m diameter. A controlled temperature gradient is created along the length of the high-temperature plasma plume. Reactants can be injected in solid, liquid, or gas form at a variety of locations (ports A, B, and C), i.e., at different temperatures. Ports D-K are for the insertion of diagnostic equipment, quench modifiers, and/or pressure-assisted purging devices. The product can be extracted manually (batch processing) or by gas purging (semi-continuous). The BNNT materials, produced at a maximum rate of 35 g/hr, comprise nano-ribbons, nano-cocoons, and nano-capsules [ref. 12].

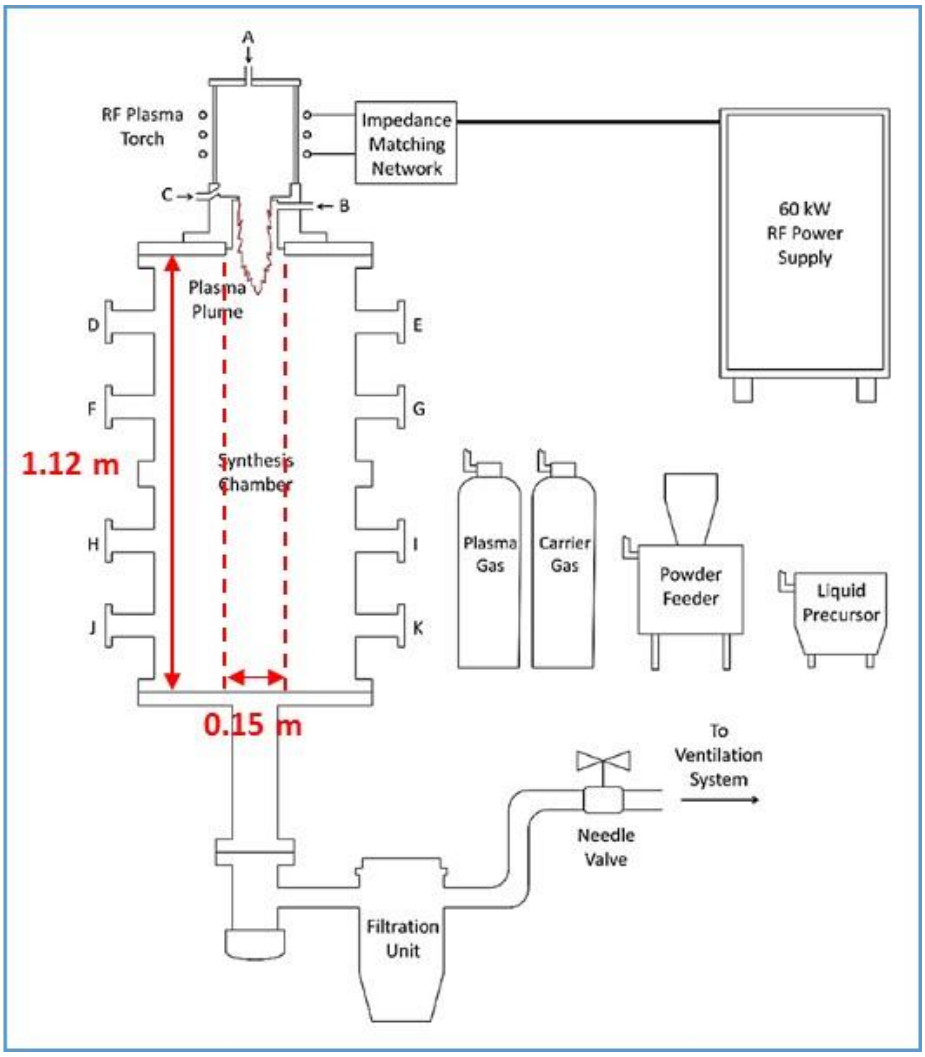

Figure 2. The facility developed at the University of California – Berkeley for RF plasma synthesis of BNNTs at a production rate of ~35 g/hr. Processing conditions include a PL-50 Tekna torch operating at ~45 kW, a pure N_2 plasma gas, reactor pressures greater than atmosphere, and elemental B powder feedstock [ref. 12].

Synthesis conditions are selected in the ranges of 40–50 kW plasma power, 101–517 kPa chamber pressure, 50 slpm N_2 plasma gas, 2–5 slpm N_2 carrier gas, and –325 mesh ($d \leq 44$ μm), amorphous B powder at 100–1700 mg/min feed rate [ref. 12]. Example processing parameters given include

- 40 kW, 172 kPa, 50 slpm, 2.5 slpm, 150 mg/min => 9 g/hr
- 40 kW, 103–310 kPa (ramp), 50 slpm, 2.5 slpm, 246 mg/min => 14.8 g/hr

Quotation from UC-B summarizing the effort;

> The EPIC system immediately generates a fibrous, light-colored, cotton-candy web-like material, which soon occupies the entire cross-sectional area of the synthesis chamber. The material initially accumulates in the upper half of the chamber, and as the run is

continued, the synthesis chamber gets successively packed, filling half the total chamber volume in approximately 30 min. In conjunction with fibrils packing the interior volume of the synthesis chamber, the chamber walls typically also become coated in a similarly light colored material, which can be easily peeled off as a continuous felt-like film. Both the (cotton-candy-like) fibril, and (felt-like) sheet materials are predominantly composed of pure BNNTs. The lower density material consists of mm to cm bundles, with rough macroscopic alignment of the fibrils. [ref. 12]

1.1.2. National Research Council – Canada (NRC-C)

The facility developed at NRC-C, now referred to as the hydrogen-assisted BNNT synthesis (HABS) system, is shown in figure 3 [refs. 14 and 15]. The facility also consists of a 60 kW Tekna RF torch mounted on top of a "stove-pipe" reaction/quenching chamber, coupled with filtration devices, and a vacuum system. The internal dimensions of the graphite-lined reactor are ~1 m long by ~0.15 m diameter. The NRC-C effort is also a redirection of methodology developed earlier for continuous production of single-walled CNTs using RF plasma synthesis techniques [refs. 16 and 17]. Employing a similar processing philosophy to BNNT production, the best results are obtained when hexagonal boron nitride (h-BN) powder is used as feedstock, the plasma forming gas is a ternary mixture of Ar, N_2, and H_2, and the plasma chamber is operating at close to atmospheric pressure. A variety of BNNT-containing products have been generated at a combined rate of up to 20 g/hr [ref. 15].

Synthesis conditions are selected in the ranges of 35–60 kW plasma power, 91–101 kPa chamber pressure, 100–120 slpm Ar/N_2/H_2 sheath gas, 30 slpm Ar central gas, 3 slpm Ar carrier gas, and –50–100 nm h-BN (or B) powder at 500 mg/min feed rate [ref. 14]. Examples of the given processing parameters include

- 35 kW, 96 kPa, 45/55/20 slpm, 30 slpm, 3 slpm, 500 mg/min => 6.3 g/hr
- 35 kW, 96 kPa, 25/55/30 slpm, 30 slpm, 3 slpm, 500 mg/min => 20 g/hr

Quotation from NRC-C summarizing the effort;

> BNNT material grown by the HABS process exhibits three distinct macro-morphologies depending on where and how it deposits within the reactor. Entangled fibrils, macroscopic cloth-like sheets, and very low density cotton-like deposits are formed as a result of gas-flow-driven segregation. Microscopically, all of the products predominantly consist of small diameter (~5 nm), few-walled, and highly crystalline BNNTs. [ref. 15]

Of the two approaches, the UC-B method is attractive because of its simplicity, i.e., using coarse, pure B feedstock and pure N_2 as the plasma gas. But, the best BNNT yields (35 g/hr) are associated with reactor pressures of greater than 1 atmosphere. Therefore, the approach is not compatible with the sub-atmospheric chamber at the Langley Research Center (LaRC). However, the processing details which lead to a higher production rate than the NRC-C method may prove beneficial.

The reaction chamber and filtration systems are rapidly clogged with product using either the UC-B or the NRC-C method, as shown in figure 4 [refs. 12, 15, and 18]. The need for a user-friendly BNNT material exists, i.e., a predominantly macroscopic product form which can be

continuously extracted and sorted during the actual synthesis process. The bulk of the BNNT material rapidly accumulates in reactors (figure 4(i) and Figure 5(ii)) [refs. 12 and 15] and/or filters (figure 4(iii)) [ref. 12]. The predominantly fibril-like product is extracted manually, resulting in a tangled mass of material, as shown in figure 4(iv) [ref. 15]. Considerable post-processing, typically using wet separation techniques, is required to obtain a usable product [e.g., ref. 19]. The fact that mass quantities of BNNTs have not been available until recently somewhat negates this issue. However, there is obviously room for improvement for structural material applications. It is suggested that if BNNTs can be produced in "cotton candy"-like form, then many of the continuous, dry processing techniques common in the cotton and microfiber industries may be utilized, e.g., alignment by conventional or electrostatic carding [e.g., ref. 20].

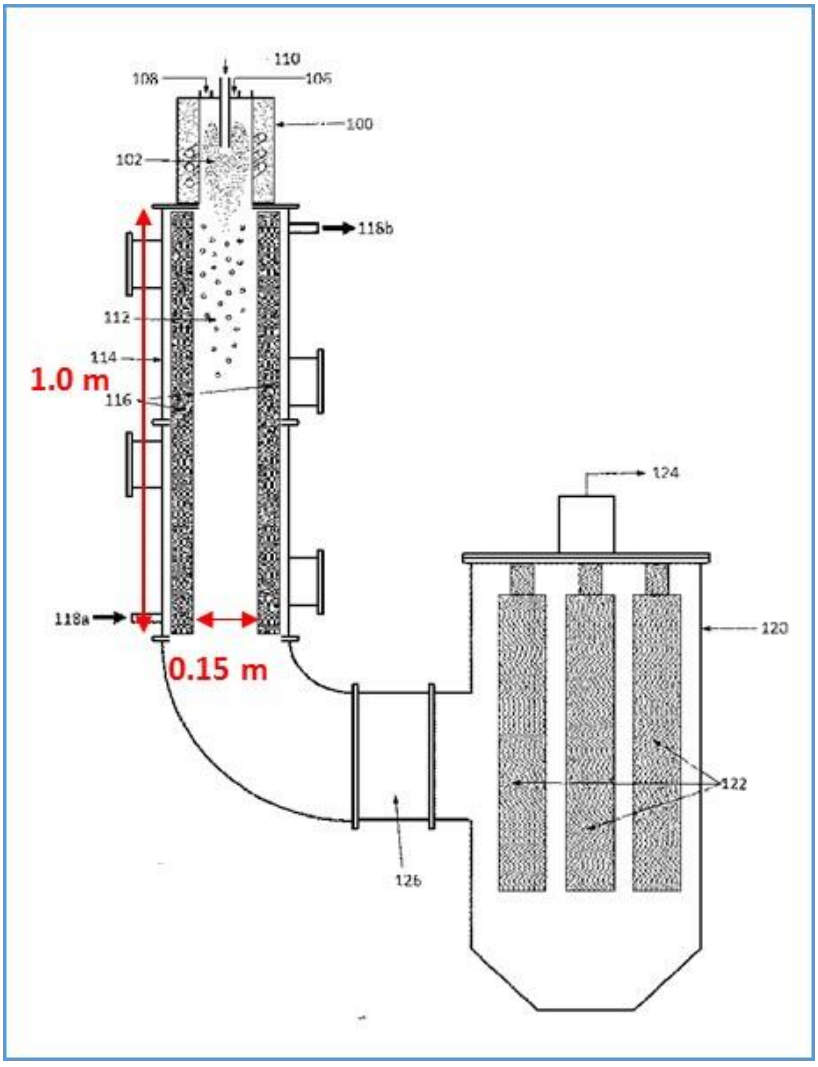

Figure 3. The facility developed at the National Research Council – Canada for the RF plasma synthesis of BNNTs at a production rate of ~20 g/hr. Processing conditions include a PL-50 Tekna torch operating at ~35 kW, an Ar/N_2/H_2 plasma gas mix, reactor pressures less than atmosphere, and BN powder feedstock [ref. 14].

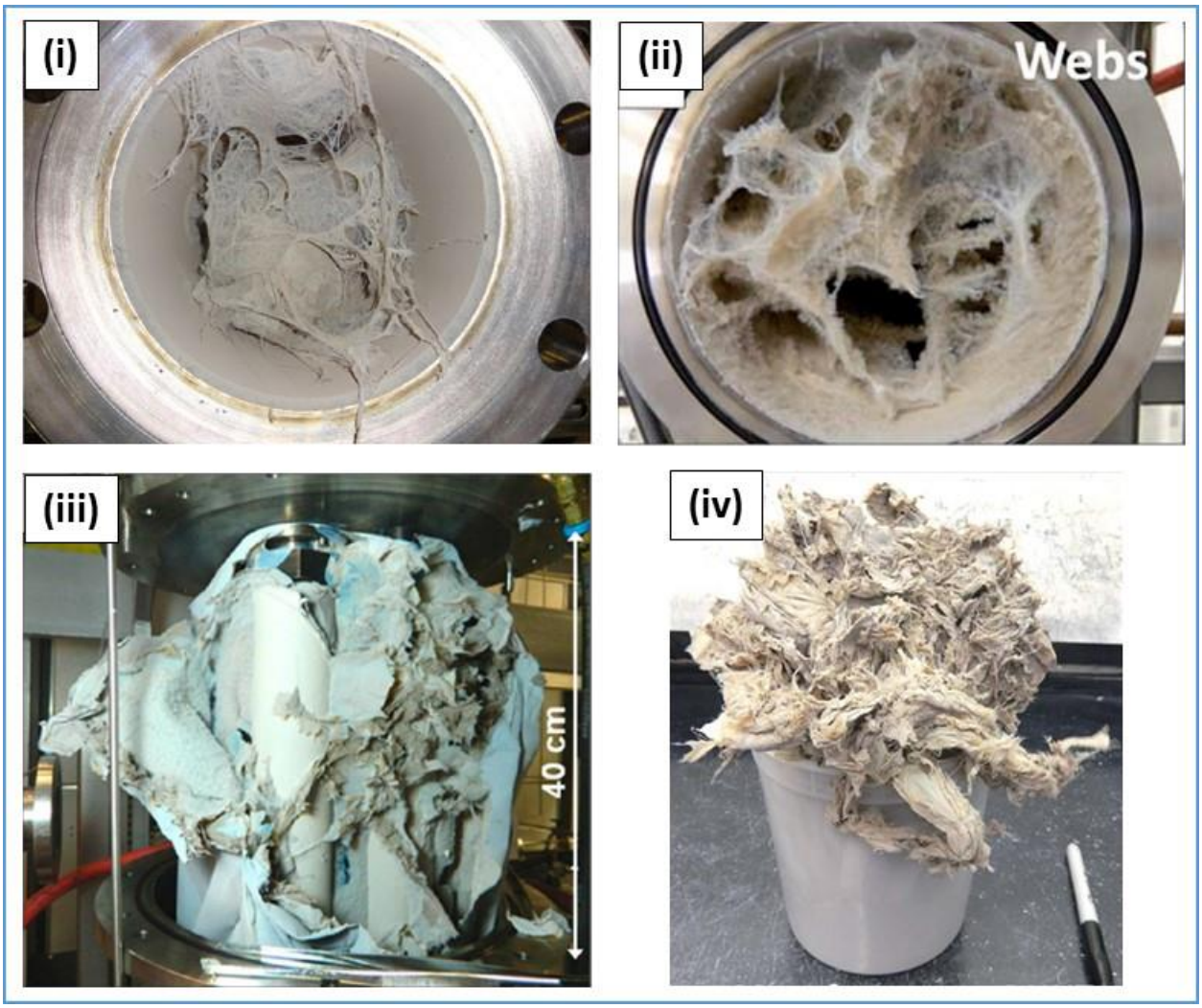

Figure 4. Accumulation of bulk product during the incumbent RF plasma synthesis processes: (i) in the UC-B reactor [ref. 12]; (ii) in the NRC-C reactor [ref. 15]; (iii) in the NRC-C filtration system [ref. 18]; and (iv) BNNT materials weighing ~20 g, manually extracted from the NRC-C filters [ref. 15].

Both the UC-B and the NRC-C methods generate material with three distinct morphologies which possess a high BNNT content [refs. 12 and 18]. The color of the as-grown products has a grayish hue which transforms to snow white following purification procedures. NRC-C has demonstrated that the structural quality of the BNNT is the same within these different materials; only the macroscopic morphologies differ. The lengths of the BNNTs are estimated at a few microns, based on more detailed analyses of small samples [ref. 18]. The images shown in figure 5 indicate that the major difference between the various BNNT materials is the density. Figure 5(i) shows that the fibril-like materials appear as bundles of "fibers," and BNNT yarns can be drawn directly from them. Figure 5(ii) shows that the fibrils are composed of agglomerated micron-sized strands, displaying coarse alignment along the fibril axis. Figure 5(iii) shows that the cloth-like sheets have a multilayered structure, and thin diaphanous membranes can be peeled off [ref. 18]. Figure 5(iv) shows that the cloth-like materials show

randomly oriented BNNTs along with non-tubular materials that have been identified as h-BN fragments. Figure 5(v) shows that the cotton candy-like deposits have a low density, and cover the entire wall of the filtration chamber. Figure 5(vi) shows that the fluffy materials consist of widely-dispersed BNNTs and some non-tubular materials, also characterized as h-BN fragments [ref. 18].

The success of the NRC-C effort in producing large quantities of BNNTs has recently led to the technology being licensed by a commercial vendor. The following public releases of information attest to the progress that has been made towards mass production;

- Press release, August 27, 2014: NRC makes world-first demonstration of pilot-scale boron nitride nanotube production; "With the breakthrough demonstration of the world's first pilot-scale production of boron nitride nanotubes, the National Research Council of Canada (NRC) has unlocked an advanced material to drive high-value manufacturing in Canada" [ref. 21].
- Patent filing, October 23, 2014: Canadian patent application, PCT/CA 2014/050340; "Boron nitride nanotubes and process for production thereof," Keun Su Kim, Christopher T. Kingston, and Benoit Simard, National Research Council of Canada, Ottawa, Ontario, CA [ref. 14].
- Press release, May 27, 2015: Tekna launches a revolutionary material on the market: boron nitride nanotubes; "Tekna Holdings Canada Inc. has entered into an exclusive agreement with the National Research Council of Canada (NRC) to allow the firm to manufacture BNNTs in commercial quantities using a process developed by NRC on a Tekna machine" [ref. 22].

1.2. Technical Overview

One feature that the UC-B, NRC-C and LaRC efforts have in common is that a RF torch manufactured by Tekna Plasma Systems, Inc., Sherbrooke, QC, Canada, is employed. Examples of the different sizes of torch produced and a schematic of the typical internal configuration are shown in figure 6 [refs. 23 and 24]. The inductively-coupled torches are available in power ratings ranging from 30 to 200 kW in the same configuration. Tekna also offers a complete range of torches for industrial customers with power levels extending up to 1 MW, as illustrated in figure 6(i) [ref. 23]. The anatomy of a Tekna RF torch consists of four basic elements: induction coil, confinement tube(s), injection probe, and gas distributor head, as shown in figure 6(ii) [ref. 24]. The water-cooled coil, which has a proprietary configuration, generates the RF field responsible for ionizing the incoming gases and creating the thermal plasma. The outer and inner confinement tubes effectively corral the plasma and are fabricated from silicon nitride and quartz, respectively. A water-cooled, double-walled injection probe allows for the introduction of powder feedstock along the central axis of the plasma. The vertical height of this probe is adjustable within the discharge zone, which allows for more precise control of the initial thermal exposure of the injected feedstock, i.e., heating rate and total heat input [ref. 25]. The powder feedstock enters the center of the plasma on an axial trajectory, is heated very rapidly, and is propelled towards the reaction chamber.

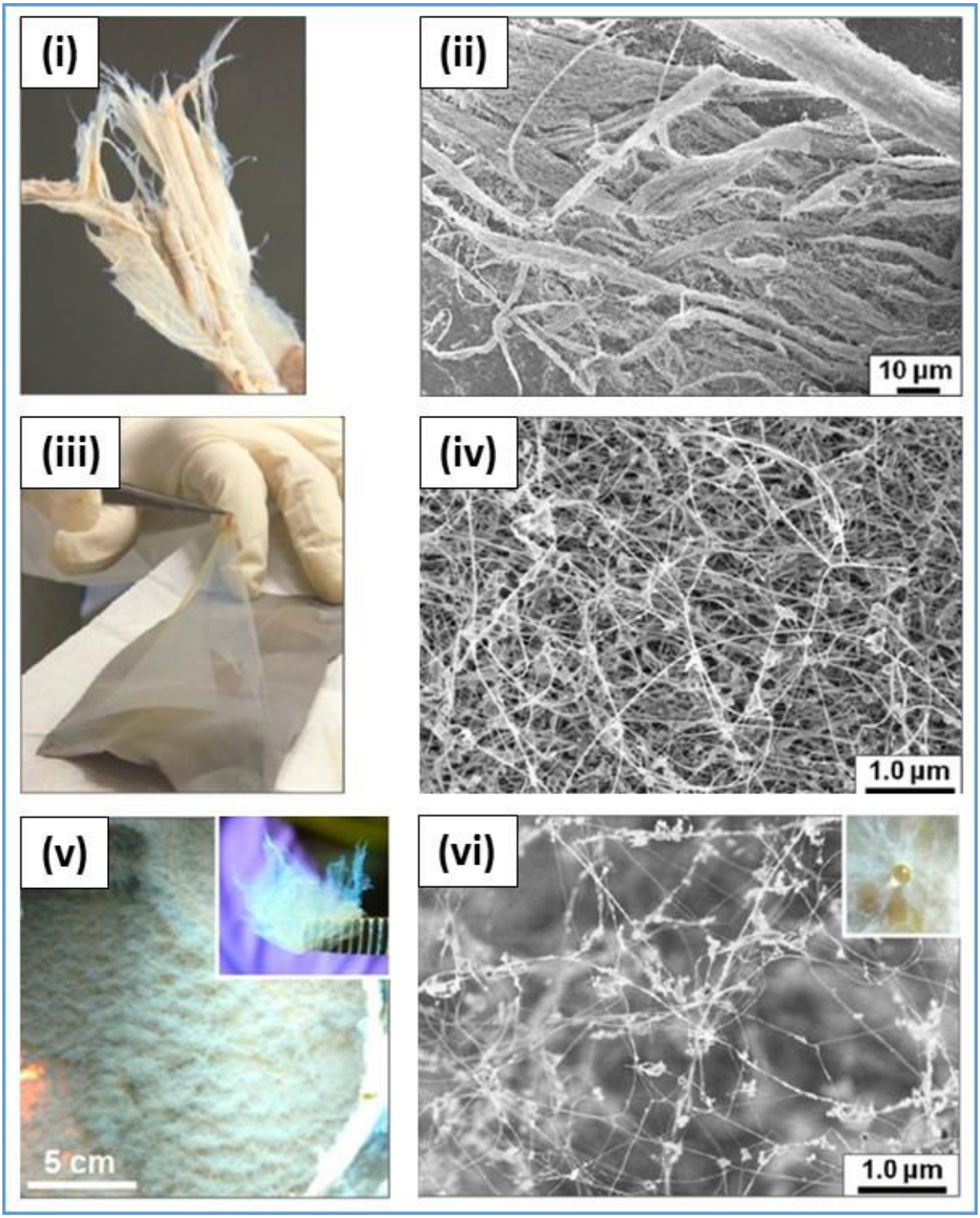

Figure 5. The varying macroscopic and microscopic characteristics of BNNT materials produced via the NRC-C synthesis process: (i) & (ii) the fibril-like morphology; (iii) & (iv) the cloth-like morphology; and (v) & (vi) the cotton candy-like morphology [ref. 18].

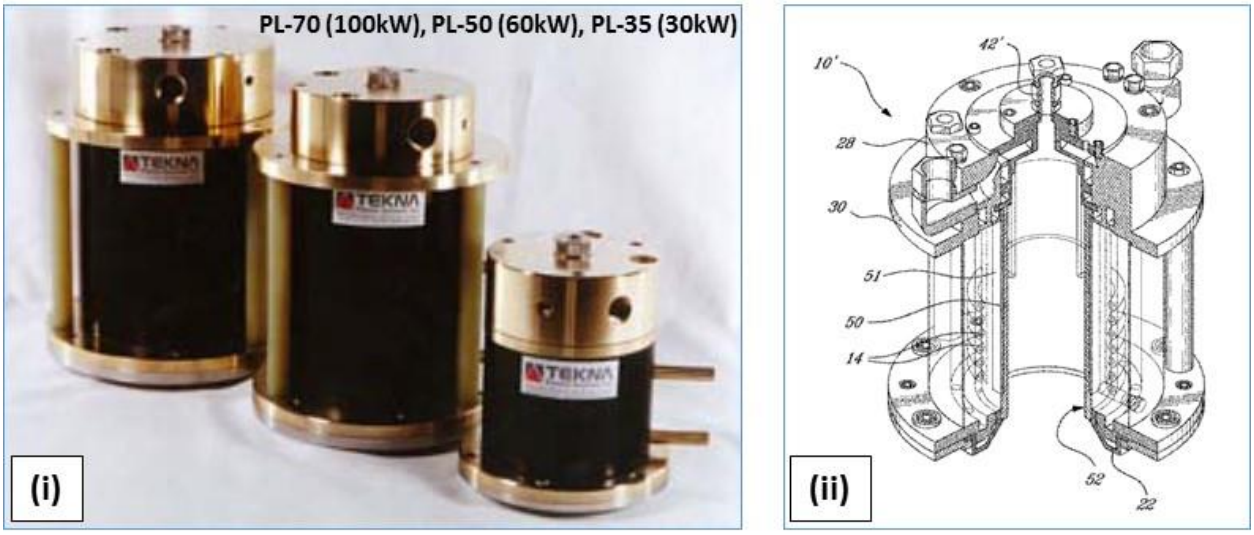

Figure 6. Induction plasma torches manufactured by Tekna Plasma Systems, Inc.: (i) three different sized torches—model number refers to internal diameter in mm [ref. 23]; (ii) schematic cutaway showing interior design of a typical RF torch [ref. 24].

Figure 7 shows the results from thermo-fluid models employed by Tekna to calculate the temperature distribution within two RF torches operating under different conditions [ref. 23]. Figure 7(i) shows a PL-50 torch operating at a power of 70 kW with a reactor pressure of 28 kPa. The plasma forming or central gas flow comprises 20 slpm Ar. The reactant or sheath gas flow is composed of 120 slpm Ar, plus 10 slpm H_2. Figure 7(ii) shows a PL-70 torch operating at a power of 100 kW with a reactor pressure of 101 kPa. The plasma forming or central gas flow comprises 40 slpm Ar. The reactant or sheath gas flow is composed of 180 slpm Ar, plus 10 slpm H_2. In both scenarios, the carrier gas flow and powder feed is zero. The peak temperature within the discharge zone is ~12,000 K in the proximity of the injector probe tip, and the temperature at the centerline of the torch nozzle is in excess of 10,000 K [ref. 23]. These bracket the conditions which might be expected during operation of the PN-70 Tekna torch installed in the LaRC radio frequency plasma spray (RFPS) facility. Both the peak temperature in the torch and the plasma temperature entering the reaction chamber are expected to be comparable for this effort.

In the incumbent processes at UC-B and NRC-C, the temperature at the entrance and exit of the reactor is critical to the transformation reactions occurring within [refs. 12 and 18]. Numerical modeling is a necessity in the absence of diagnostic devices that can directly measure the very high temperatures involved [ref. 26]. Thermocouple data gathered from exterior surfaces can be used as input to create vertical thermal profiles of the reaction zone. Figure 8 shows the results of NRC-C modeling to calculate the temperature distribution in a BNNT reactor under specific synthesis conditions [refs. 27 and 28]. A schematic of a 60 kW Tekna torch mounted atop the 1 m long reaction chamber is shown in figure 8(i) [ref. 27]. The exterior temperatures are monitored by type C (T_{max} = 2500 K) thermocouples in the upper half of the chamber, and by type K (T_{max} = 1500 K) in the lower half and exhaust.

Figure 8(ii) shows the thermal profile within the reaction chamber under operating conditions typically used for BNNT synthesis [ref. 28]. The right hand side shows the region in the reaction

zone where the temperature is ≥4000 K. The net plasma power is 35 kW with a reactor pressure of 93 kPa. The gas flow rates for the carrier and central gases are 3 slpm and 30 slpm of Ar, respectively. The sheath gas flow rate is 120 slpm, comprising 45 slpm Ar, 55 slpm N_2, and 20 slpm H_2. The NRC-C model reveals that the peak temperature in the torch is ~11,000 K. Along the central axis, the temperature drops from ~9000 K to ~2000 K within the 1 m long reactor, and remains above 4000 K for the first ~40 cm. The significance of this is that the boiling point of elemental B is 4200 K at atmospheric pressure, and it is effectively a vapor above this temperature [ref. 29]. The temperature at the bottom of the reactor is significant because the melting point of elemental B is 2349 K at atmospheric pressure [ref. 29]. Liquid B droplets solidify at this temperature and any reactions with other gaseous reactants are severely curtailed.

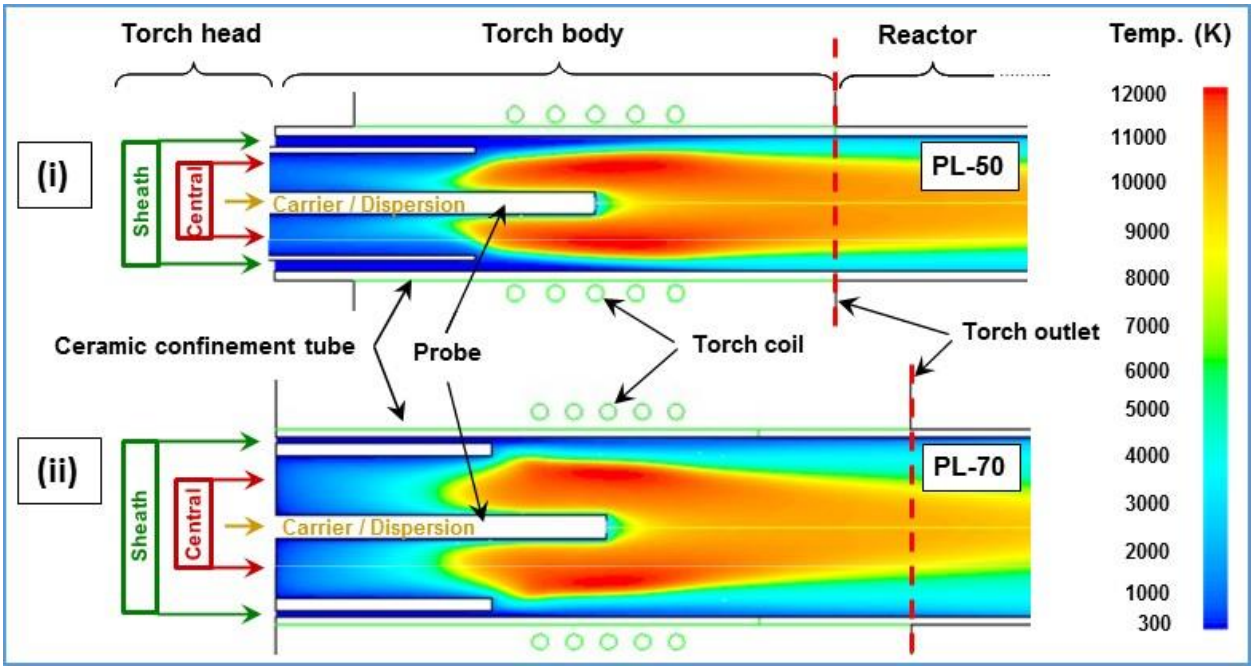

Figure 7. Tekna modeling of thermal profiles within a PL-50 and PL-70 torch under representative operating conditions: (i) power = 70 kW, reactor pressure = 28 kPa, carrier = 0, central = 20 slpm Ar, sheath = 120 slpm Ar + 10 slpm H_2; and (ii) power = 100 kW, reactor pressure = 101 kPa, carrier = 0, central = 40 slpm Ar, sheath = 180 slpm Ar + 10 slpm H_2 [ref. 23].

The high temperatures in the RF torch create a partially ionized gas, which comprises a mixture of molecules, atoms, electrons, and ions. N_2 and H_2 gas can undergo complete ionization in plasmas, but temperatures of 12–15,000 K are required [ref. 30]. In this case, the plasma contains the highly reactive nitrogen and hydrogen species and dense B vapors. It is evident that vaporizing BN (instead of solid B in the presence of N_2 gas) may provide the correct stoichiometry at the onset of synthesis. Ionization of monatomic Ar gas occurs directly (central gas), and diatomic N_2 and H_2 are dissociated into monatomic gases prior to being ionized into N and H radicals (sheath gas).

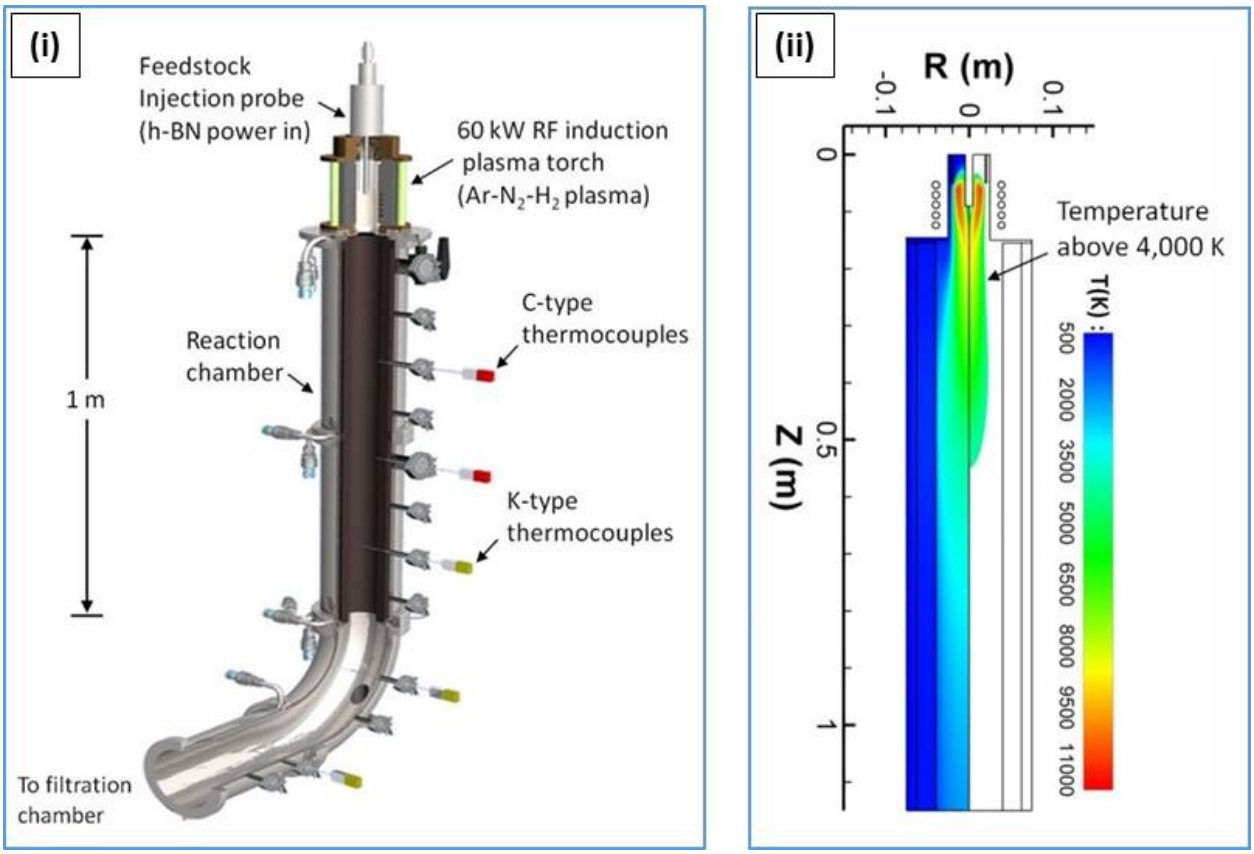

Figure 8. Thermal profiles in the NRC-C reactor: (i) exterior temperatures are monitored with Type C (T ≤ 2590 K) and Type K (T ≤ 1520 K) thermocouples [ref. 27]; and (ii) interior temperatures are calculated via numerical modeling. The right half of the profile shows the region where T ≥ 4000 K [ref. 28].

Including H_2 in the plasma forming gas composition proved critical in creating both the very high temperatures and the chemical environment appropriate for synthesis of large quantities of BNNTs. For example, increasing the H_2 content from 13 to 18 vol% caused a 30-percent improvement in production efficiency [ref. 27]. It is suggested that the presence of partially ionized H_2 gas may provide an atmosphere more conducive to the formation of BNNTs by lowering the BN decomposition temperature and also stabilizing the decomposed BN. Coupled with a controlled dual cooling rate within the extended hot zone, the net result is rapid nucleation and prolonged growth of BNNTs.

NRC-C subscribes to the "root growth" mechanism [ref. 31], and the sequence of BNNT formation during RF synthesis is envisioned as

- dissociation of BN into B vapor and N radicals
- condensation of nano-sized B droplets
- reaction between B nano-droplets and reactive N species
- nucleation and growth of BNNTs by re-nitriding of B

The hypothesis is that the droplets condensing from the B vapor act as seeds for BNNT formation. Subsequent interactions with reactive nitrogen radicals, such as N, N^+, and N_2^+, in a decreasing temperature gradient cause BNNT growth. The thermal profiles set up in the reactor prior to introduction of feedstock govern the size of the BNNTs produced. H_2 is cited as a catalyst because its presence stabilizes the radicals and extends the growth regime [ref. 27.

Figure 9 illustrates the relationship between the controlled thermal profile and a correlation with the reactions involved in the formation of BNNTs [refs. 27 and 28]. A detailed view of the thermal profile created within the reactor is shown in figure 9(i) [ref. 27]. It is evident that there are two distinct cooling regimes which serve separate functions. The initial gradient stating at the reactor entrance and extending ~40 cm down the reactor has a cooling rate of ~10^5 K/s. The final temperature gradient extending through the remainder of the reactor to the exit has a cooling rate of ~10^3 K/s. Figure 9(ii) reveals that the peak temperature in the RF torch controls the extent of B vaporization and N_2 ionization, which ultimately governs the yield of BNNTs [ref. 28]. The initial thermal gradient controls the size of the B droplets, which governs BNNT nucleation. The final thermal gradient over the remainder of the reactor determines the longevity of the molten droplets, which governs BNNT growth.

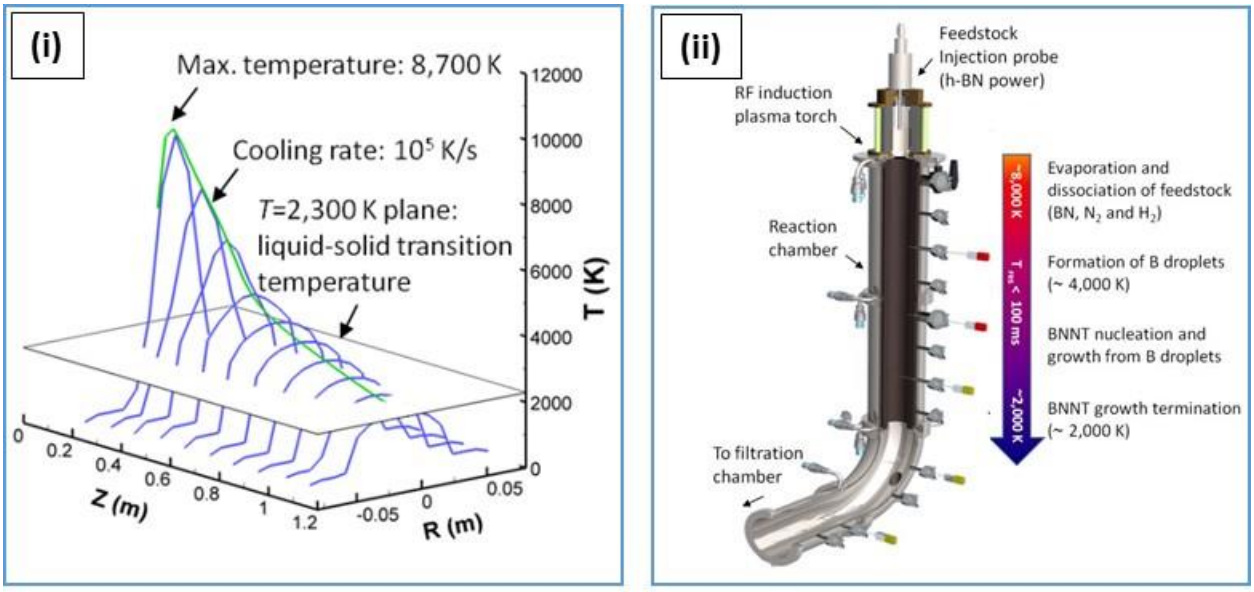

Figure 9. Location of reactions in the NRC-C chamber: (i) peak temperature and dual temperature gradients govern regions of vaporization, condensation and solidification of pure boron [ref. 27]; and (ii) dissociation of BN feedstock at T ~8000 K, formation of B droplets at T ~4000 K, BNNTs nucleate and grow in ~100 ms, BNNT growth ceases at T ~2000 K [ref. 28].

2. Experimental Philosophy

The prime objective is the allotropic transformation of h-BN powder into high quality BNNTs in an atmosphere charged with nitrogen species. A key step in the synthesis process is the formation of B vapor, followed by the condensation of fine B droplets. As mentioned, the liquification and vaporization temperatures for pure B metal are 2349 K and 4200 K, respectively [ref. 29]. Subsequent re-nitriding of the B droplets is accelerated by dissociation of the diatomic N_2 gas at a minimum of 7500 K [ref. 27]. Increasing to even higher temperatures causes the monatomic N to become partially ionized (reaching completion at 12,500 K) [ref. 30]. This event creates even more reactive species (N^+ and N_2^+ ions), and further promotes the transformation. As a result, the sequence of critical processing temperatures associated with using h-BN powder feedstock may be summarized as [ref. 32]

- 3246 K; BN(solid) => BN(gas) (sublimation)
- 3500 K; BN(solid) => B(liquid) + ½ N_2(gas) (decomposition)
- 4200 K; BN(solid) => B(gas) + ½ N_2(gas) (vaporization)
- 7500 K; BN(solid) => B(gas) + N(gas) (dissociation)

The operating parameters derived from the NRC-C work will be tailored to the LaRC reactor design for BNNT synthesis. Although processing parameters for the Tekna torch should be directly transferable, the geometrical configuration of the NRC-C and LaRC plasma systems differs. The UC-B (figure 2) and NRC-C (figure 3) reactors are vertically-mounted, long and narrow cylinders with a highly confined plasma plume [refs. 12 and 18]. In contrast, the expansive LaRC plasma chamber is a horizontally mounted, 1 m diameter by 1 m long chamber, as shown in figure 10. The equipment setup normally includes a ~30 cm diameter rotating/translating mandrel, which is coincident with the central axis of the chamber. The throw distance from the gun to the mandrel surface is ~53 cm, which will be retracted, or removed, for in-situ synthesis studies. In the absence of the mandrel, the throw distance from the gun exit nozzle to the bottom of the chamber becomes ~112 cm. In the NRC-C facility, the reaction zone is 1 m long with a steep temperature decrease over the first ~40 cm. The dimensions of, and residence times in, the plasma plume in the LaRC reaction chamber are commensurate with those in both of the incumbent processes. The PL-50 Tekna torches installed at UC-B and NRC-C are 50 mm in diameter and operate at a maximum power of 60 kW [refs. 12 and 18]. The PN-70 Tekna torch installed at LaRC is 70 mm in diameter and operates at a maximum power of 100 kW.

It is anticipated that the desired temperature gradient(s) can be created by utilizing the extra power and the broader confines of the LaRC chamber. Figure 11 shows that the free-flight characteristics of the plasma plume generated may be more dynamic in nature, i.e., both temperature and chemistry. Careful control of the temperature and gas composition profiles will be critical to the nucleation and growth of BNNTs. In combination, the ambient pressure of the spray chamber and the pressure of the injected forming gases govern the dimensions and temperature profile of the plasma plume shown in figure 11(i). These profiles control the heat cycle of the injected powder feedstock, i.e., maximum temperature, incremental cooling rates, and total residence time/distance. It may also be plausible to exploit the differing configuration of the LaRC reactor to more readily control the BNNT aspect ratio during synthesis.

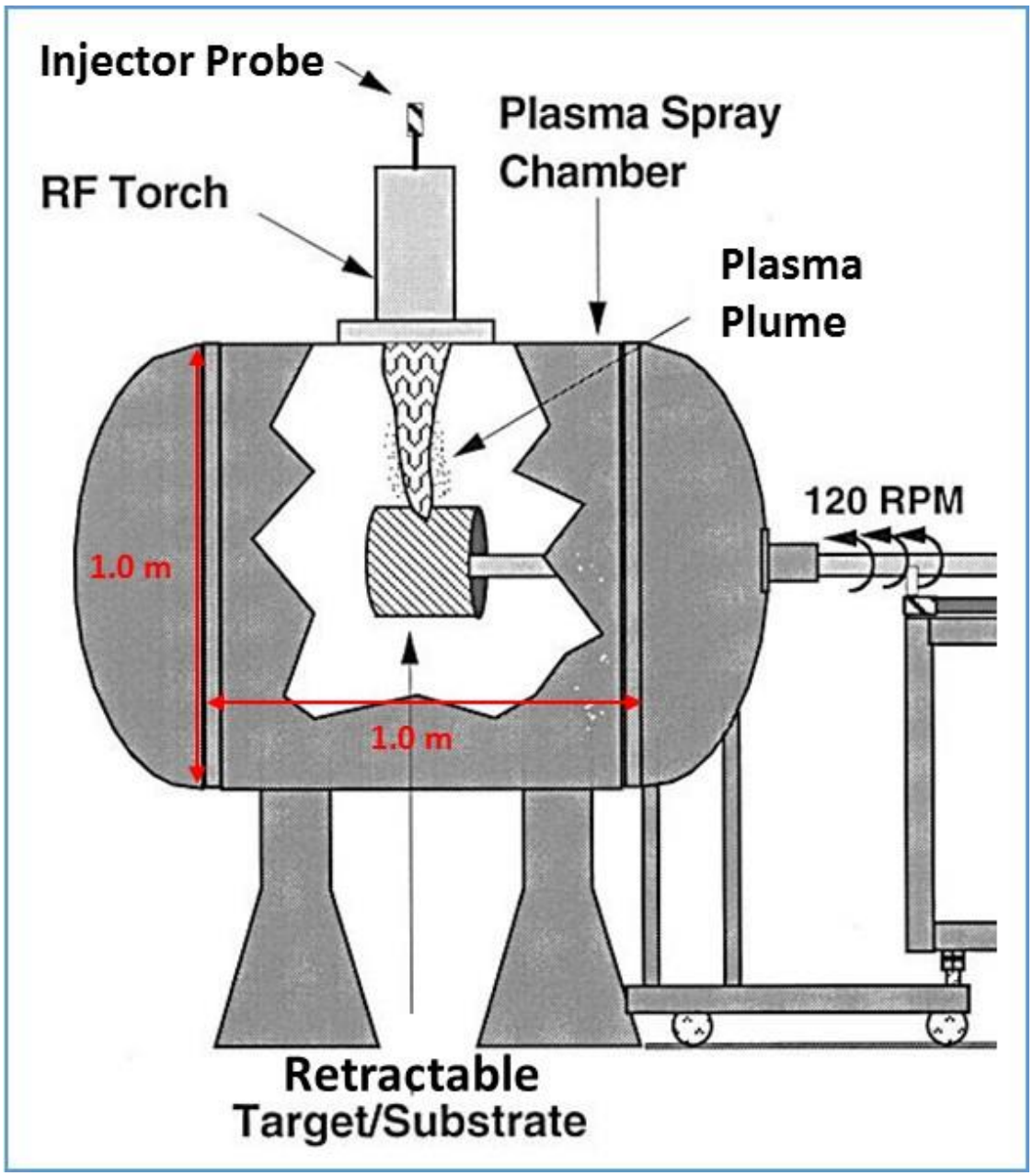

Figure 10. The RF plasma deposition facility at LaRC adapted for the in-situ plasma synthesis of BNNTs. Processing conditions include a PN-70 Tekna torch operating at ~100 kW, an Ar/N_2/H_2/He plasma gas mix, reaction chamber pressures less than atmosphere, and BN (or B) powder feedstock.

As illustrated in figure 11(ii), the success of the NRC-C process hinges on creating dual temperature gradients and establishing the key transition at 4200 K [ref. 27]. This is the minimum temperature at which elemental B exists as a vapor at pressures close to atmosphere. The hypothesis is that the faster the cooling rate, the smaller the droplets, and the smaller the diameter of the BNNTs. The subsequent slower cooling over a longer distance to 2349 K, at which remnant B droplets solidify, represents the period of BNNT growth. It is theorized that

the extent of this zone may be used to control the length of the BNNTs. In combination, these factors ultimately govern the aspect ratio of the BNNTs produced. The red dotted line illustrates a scenario where the aspect ratio of the BNNTs could be enhanced by increasing the first thermal gradient and decreasing the second thermal gradient within the same reaction zone. Very steep temperature gradients have already been achieved by radial injection of quenching gas into a RF plasma plume, as shown in figure 11(iii) [ref. 23]. As a consequence, a method for direct measurement of the plasma temperature as a function of location may prove critical to success.

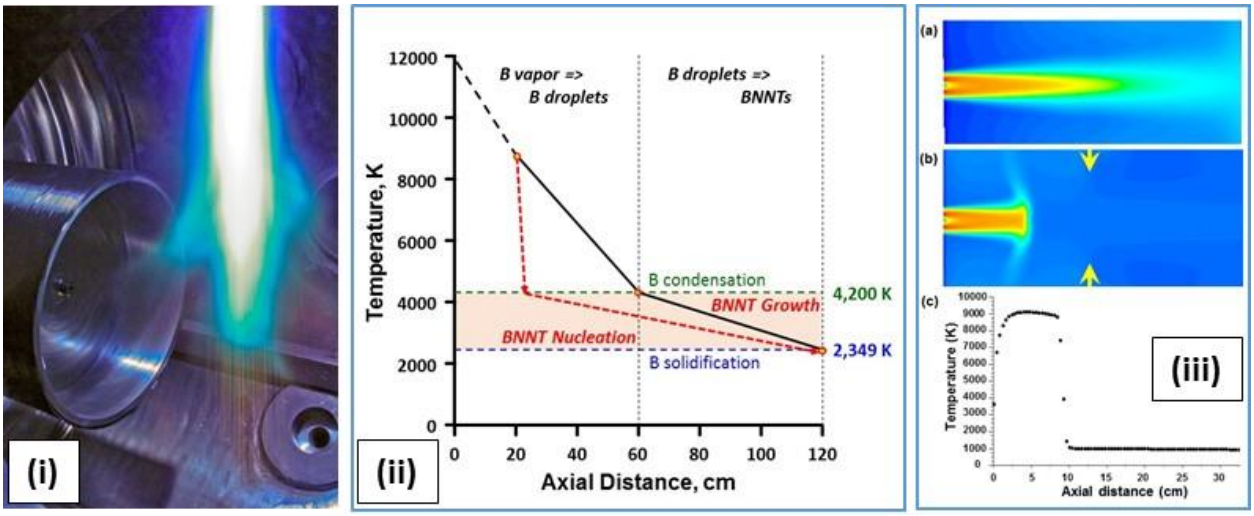

Figure 11. Controlling thermal profiles in the LaRC reaction chamber: (i) typical free-flight plasma plume (mandrel withdrawn); (ii) dual temperature gradients for high aspect ratio BNNTs, adapted from [ref. 27]; and (iii) steep gradients created by radially injected quench gas [ref. 23].

Characteristic features of the UC-B, NRC-C and LaRC activities are compared and contrasted in table 1. The use of commercially-available elemental B or BN powder feedstock in all cases is a bonus. Issues with the handling of ultra-fine, non-metallic particulate is negated by the UC-B approach. The elimination of metallic catalysts, when compared with earlier methods will be a benefit to product purity. It is evident that induction plasma techniques are efficient, as witnessed by the high proportion of BNNTs in the final product. Both the UC-B and NRC-C facilities include narrow, cylindrical reactors with filtration systems which may be a disadvantage from the perspective of product handling. The tangled nature of the bulk of the product may necessitate manual extraction and batch processing. Efforts at UC-B have demonstrated that pure N_2 alone is effective for BNNT synthesis, and H_2 may not be needed as a catalyst. The concomitant increase in potential production rates is very attractive. The Achilles heel of the UC-B approach may be the higher reactor pressures that are currently specified. The sub-atmospheric techniques of NRC-C and LaRC lead to less stringent equipment requirements, providing that H_2 is used in low volume percentages.

The use of relatively coarse, elemental B feedstock may be an advantage from the perspective of simplified processing, but there is an economic disadvantage associated. Using 70 nm BN feedstock is desirable because it represents a cost-effective option ($220 per kg). The aerosol-

grade powder is widely used as a solid lubricant, and large quantities are readily available. Thermal spray operations employ 45 µm BN feedstock in limited applications, which is a more expensive option. Thermal spray grade B powder, which sees very limited use, is the most expensive option ($2200 per kg). These factors need to be considered during process scale-up because production costs will be impacted. Any performance breakthrough must outweigh the fabrication costs associated with acreage structural materials [ref. 1].

Table 1. Characteristic features of the UC-B, NRC-C, and LaRC processes are compared and contrasted. The incumbents have some common pros and cons, as well as some separate benefits and issues. The LaRC approach has some projected advantages, but a powder feeder concern remains unresolved.

Process	Pros	Cons
Incumbents	B, BN feedstock No metal catalyst High percent BNNTs	Power = 60 kW max. Stove-pipe reactor Tangled mass product Batch processing
UC-B	Pure N_2 plasma Powder size ~ 44 µm BNNT yield ~ 35 g/h	High pressure Porous metal filters
NRC-C	Low chamber pressure BNNT yield ~ 20 g/h	Porous metal filters Powder size ~ 70 nm
LaRC	Low chamber pressure Power = 100 kW max. Expansive chamber Cyclone separator	Powder feeder

The intent of the LaRC effort is the formation of predominantly high aspect ratio BNNTs in a user-friendly form for structural material applications. As matrix reinforcing agents, uniform length, diameter, and defect count tend to be more important than crystallinity, number of walls, or chirality. Therefore, synthesis of the low density, cotton candy-like product is the target. In this macroscopic form, the opportunity to apply dry techniques for the collection, purification and fractionation (by aspect ratio) of BNNT product is increased. The 100 kW RF torch, expansive reaction chamber, and potential elimination of filters indicate that the RFPS facility is amenable to the production of large quantities of high aspect ratio BNNTs, with a target yield comparable with the incumbent processes. The planned inclusion of diagnostic enthalpy probe and dry separation methods may ultimately lead to an optimized, semi-continuous process.

3. Results and Discussion

3.1. Synthesis

Details concerning the internal workings of a Tekna RF torch are illustrated in figure 12 [ref. 24]. The cut-away schematic shows the configuration of a typical high performance induction plasma torch mounted on a reaction chamber. The height-adjustable, powder injection probe sits along the central axis of the torch. The plasma is confined within the discharge zone by a pair of concentric, cylindrical tubes. These are surrounded by an assembly consisting of a non-helical induction coil imbedded in a phenolic torch body. All of the components are water-cooled on individually-controlled circuits. The most significant feature of the Tekna torch from an experimentation perspective is the gas distribution system. The torch head delivers three distinct gas streams into the discharge zone, which combine to define both the plasma temperature and the reaction atmosphere. Each of the gas streams can be controlled independently and may comprise a single gas, or a mixture of gases.

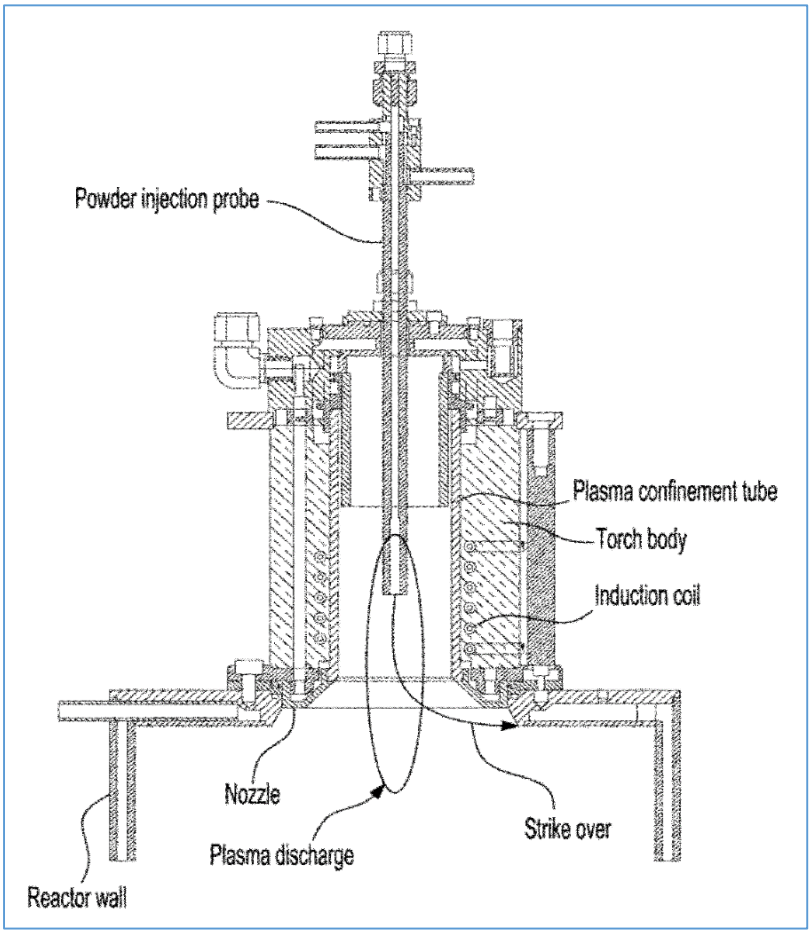

Figure 12. A schematic showing the inner workings of RF torches manufactured by Tekna Plasma Systems, Inc. The basic components of the latest iteration of the design are indicated. An innovative feature is the use of non-helical induction coils [ref. 24].

Figure 13 illustrates how the various inlet gases combine in the discharge zone to create the very hot plasma by inductive coupling [ref. 33]. The carrier gas transports solid (or liquid) reactants into the center of the plasma via the injection probe. The central gas enters the torch chamber directly in a tangential, swirling motion between the injector probe and the inner confinement tube. The gas, or mixture of gases, is the first to ionize in the induction zone, and is commonly referred to as the plasma-forming gas. The sheath gas is introduced through an annulus of nozzles in the torch head located between the outer (ceramic) and inner (quartz) confinement tubes. Creating either a vortex or columnar flow pattern, the traditional functions of this gas are twofold; (i), to stabilize the plasma discharge; and (ii), to protect the confinement tubes (by cooling) [ref. 34]. In this case, it serves the equally important function as a vehicle for inserting the reactant gases as a specified volumetric mixture. For most purposes, the carrier and central gas streams are a low rate feed of pure Ar, and the sheath gas is a high rate feed of mixed gases [ref. 34]. The sheath gas mixture can contain Ar, He, H_2, and/or N_2, depending on plasma temperature and processing chemistry targets. Careful metering of the individual inputs dictates the blended gas composition and ultimately governs the temperature and reactions occurring within the plasma.

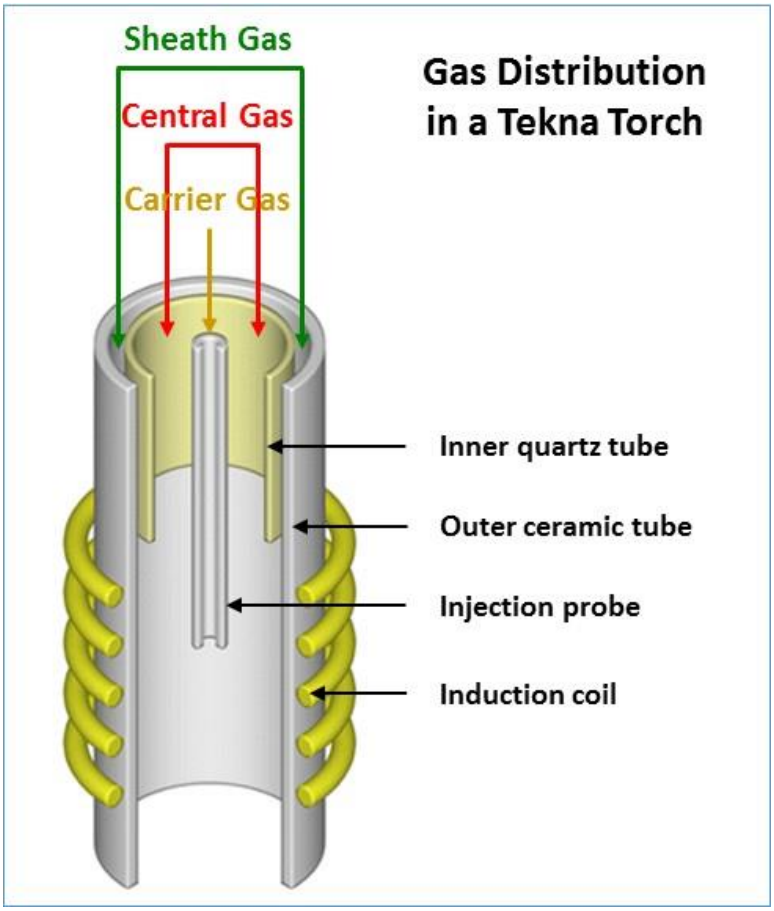

Figure 13. The distribution of gases emanating from the head of a typical Tekna RF torch are shown [ref. 33]. The individual carrier, central, and sheath gas streams blend in the discharge zone, where the inductively-coupled plasma is created and accelerated.

The methodology pioneered by NRC-C for mass production of BNNTs is best suited to the low pressure, high volume RFPS facility located at NASA LaRC. In addition, both facilities employ a Tekna RF plasma torch, such that the operating parameters are compatible. Although the NRC-C "recipe" is proprietary, detailed information has been extracted from the public domain [refs. 14, 27, and 28]. Chronological development of the process parameters for BNNT synthesis is captured in table 2 [ref. 3]. The plate power, reaction chamber pressure and feedstock characteristics have remained unchanged. Evidently, NRC-C optimized these particular process variables during earlier efforts. The percentages of Ar, N_2, and H_2 are presented as a fraction of the entire gas volume entering the Tekna torch. The flow rates of pure Ar for both the carrier and central gases remain unchanged. Only the sheath gas composition has been adjusted in order to increase the yield of BNNTs from 21% to 67%, based on a feed rate of 0.5 g/min [ref. 27]. It is apparent that the main difference between the early and late recipes is the H_2 content, with a proportionate decrease in the Ar content. Again, subscribing to the root growth mechanism, the H_2 is believed to act as a catalyst by extending interaction between reactive nitrogen species and pure B droplets [ref. 31].

Table 2. Many of the process parameters developed by NRC-C for RF plasma synthesis of BNNTs were established early. The plasma gas compositions are presented as a percentage of the total gas volume introduced. Only the sheath gas has been adjusted to increase the yield [ref. 14].

NRC-C Parameters		Early Recipe (2012-13)	Late Recipe (2014-)
Plasma Power		35 kW	35 kW
Chamber Pressure		101 kPa	101 kPa
Carrier Gas	Argon	2.0%	2.0%
Central Gas	Argon	19.6%	21.0%
Sheath Gas	Argon	29.4%	17.5%
	Nitrogen	36.0%	38.5%
	Hydrogen	13.0%	21.0%
BN Feedstock	Size	70 nm	70 nm
	Rate	0.5 g/min	0.5 g/min
BNNT Yield		6.3 g/hr (21%)	20 g/hr (67%)

The first order of business at LaRC was to convert a system configured for metal deposition using Ar/He plasma gas to one suitable for in-situ synthesis using $Ar/N_2/H_2$ plasma gas. Preliminary experimentation assessed the performance of the facility under processing conditions representative of BNNT synthesis. It was recognized that operating parameters would differ from NRC-C due to the equipment configuration, i.e., the higher power plasma torch and expansive reaction chamber. It was surmised that gas volumes and flow rates needed to be higher than NRC-C for plasma stability. It was determined that a mixture of gases, selected from Ar, N_2, H_2, and He, might be required for each of the three main inputs. The number of gas flow controllers was increased to 8, allowing for 2 on the carrier gas, 2 on the central gas, and 4 on the sheath gas feeds. The capacity of the individual controllers was also increased to 200 slpm to account for the larger 100 kW torch.

After the extensive modifications were implemented, it was discovered that initiating and sustaining a N_2–based plasma was not trivial in the LaRC facility. It was established that the NRC-C processing conditions could be used on a percentage basis only, and the actual gas flow rates needed to be much higher. It was also observed that the plasma created was unstable at chamber pressures above 53 kPa, and the system performed most efficiently at 33 kPa. In addition, the LaRC powder feeder (PF) was designed for handling ~100 μm metal powders at relatively high feed rates. The feedstock options procured for this activity comprised thermal spray grade (99.9% pure) ~40 μm pure B and ~30 μm BN, and less expensive aerosol lubricant grade (99.5% pure) ~70 nm BN. It was recognized that very fine, low conductivity particulate is susceptible to high cohesion and bridging, particularly at low feed rates. Consequently, anti-static feed lines and rudimentary PF vibrators were installed as an initial precaution.

Table 3 shows the variables which were adjusted during the more formal plasma synthesis trials. The basic parameters are plasma torch power, reaction chamber pressure, plasma gas composition, and precursor powder characteristics. The process settings for the six LaRC trial runs are listed and compared with the two NRC-C recipes which were adopted as baselines [ref. 14]. The difference between the NRC-C baselines stems from increasing the H_2 content of the whole plasma gas from ~13 to ~21 vol%, which dramatically increased the yield of BNNTs [ref. 27]. Using these chronological improvements as a guide, the varying objectives of the individual LaRC trials are listed below;

- **LPS263**: a starting point; designed to mimic the NRC-C early recipe. This was the first successful run operating with an $Ar/N_2/H_2$, instead of an Ar/He, mixture as the plasma gas.
- **LPS264**: climbing the learning curve; designed to approach the NRC-C late recipe. During this run, it was established that the H_2 flow rate is limited to 48 slpm. Therefore, the proportion of the other gases was adjusted accordingly in order to better align with the NRC-C late recipe (on a percentage basis).
- **LPS265**: gaining experience; designed to mimic the NRC-C late recipe. Subsequent trials were designed to isolate the effect of different variables on the synthesis process.
- **LPS266**: addressing PF issues; changed from thermal spray grade to aerosol grade BN feedstock a la NRC-C recipes. During this run, lack of feed rate control came to the forefront.

- **LPS267**: incorporating He in the central gas; designed to increase plasma stability, and assess the potential to use higher chamber pressures.
- **LPS268**: incorporating He in the central and carrier gas; designed to increase plasma stability, and return to thermal spray grade metallic powders to reduce PF issues.

Figure 14 shows what the LaRC reaction chamber looks like after a typical 15-minute trial run and the product extracted. Figure 14(i) shows the interior of the whole reaction chamber at the conclusion of one of the trial runs. Figure 14(ii) is a close-up view of the bottom of the chamber, where a substrate foil was placed directly beneath the RF torch to collect product. Figure 14(iii) shows the materials manually extracted from the chamber floor, the chamber walls and the substrate. Figure 14(iv) shows that the quantity of material produced so far is very small. The macroscopic appearance of the product tends to be low density, but much denser than the cotton candy consistency desired. The weight of product should be commensurate with the feed rate, since the desired reaction comprises a simple allotropic transformation. Therefore, at 0.5 g/min for 15 minutes, there should be ~7.5 g of product. The product yield from each trial run has been less than 1 g, even accounting for exhaust losses. During most of these trials, strobing of the plasma plume was observed, which experience suggests is indicative of uneven powder feeding.

Table 3. The process variables included in the LaRC synthesis trials are presented in sequence. The basic parameters are plasma torch power, reaction chamber pressure, plasma gas composition and precursor powder characteristics. The various processing conditions employed are compared with the early and late NRC-C recipes, which were used for guidance [ref. 14].

	Plate Power kW	Chamber Pressure kPa	Carrier Gas slpm		Central Gas slpm		Sheath Gas slpm			Powder Feedstock			
			Ar	He	Ar	He	Ar	N_2	H_2	Comp.	Purity %	Size	Rate g/min
NRC-C Early	35	96	3		30		45	55	20	BN	99.5	70 nm	0.5
Vol.%			*2.0*		*19.6*		*29.4*	*36.0*	*13.0*				
LPS 263	100	33	2.6		45		90	105	40	BN	99.9	30 µm	0.5*
Vol.%			*0.9*		*15.9*		*31.8*	*37.2*	*14.2*				
NRC-C Late	35	96	3		30		25	55	30	BN	99.5	70 nm	0.5
Vol.%			*2.0*		*21.0*		*17.5*	*38.5*	*21.0*				
LPS 264	100	33	2.6		45		45	100	48	BN	99.9	30 µm	0.5*
Vol.%			*1.1*		*18.7*		*18.7*	*41.6*	*20.0*				
LPS 265	100	33	2.6		30	13	40	88	48	BN	99.9	30 µm	0.5*
Vol.%			*1.2*		*13.5*	*5.9*	*18.1*	*39.7*	*21.7*				
LPS 266	100	33	2.6		45		45	100	48	BN	99.5	70 nm	0.5*
LPS 267	100	33	2.6		30	13	40	88	48	BN	99.5	70 nm	0.5*
LPS 268	100	33		11.8	30	13	40	88	48	B	99.9	40 µm	0.5*

** Target feed rate only; actual rate much lower due to powder feeder issues (Section 3.1)*

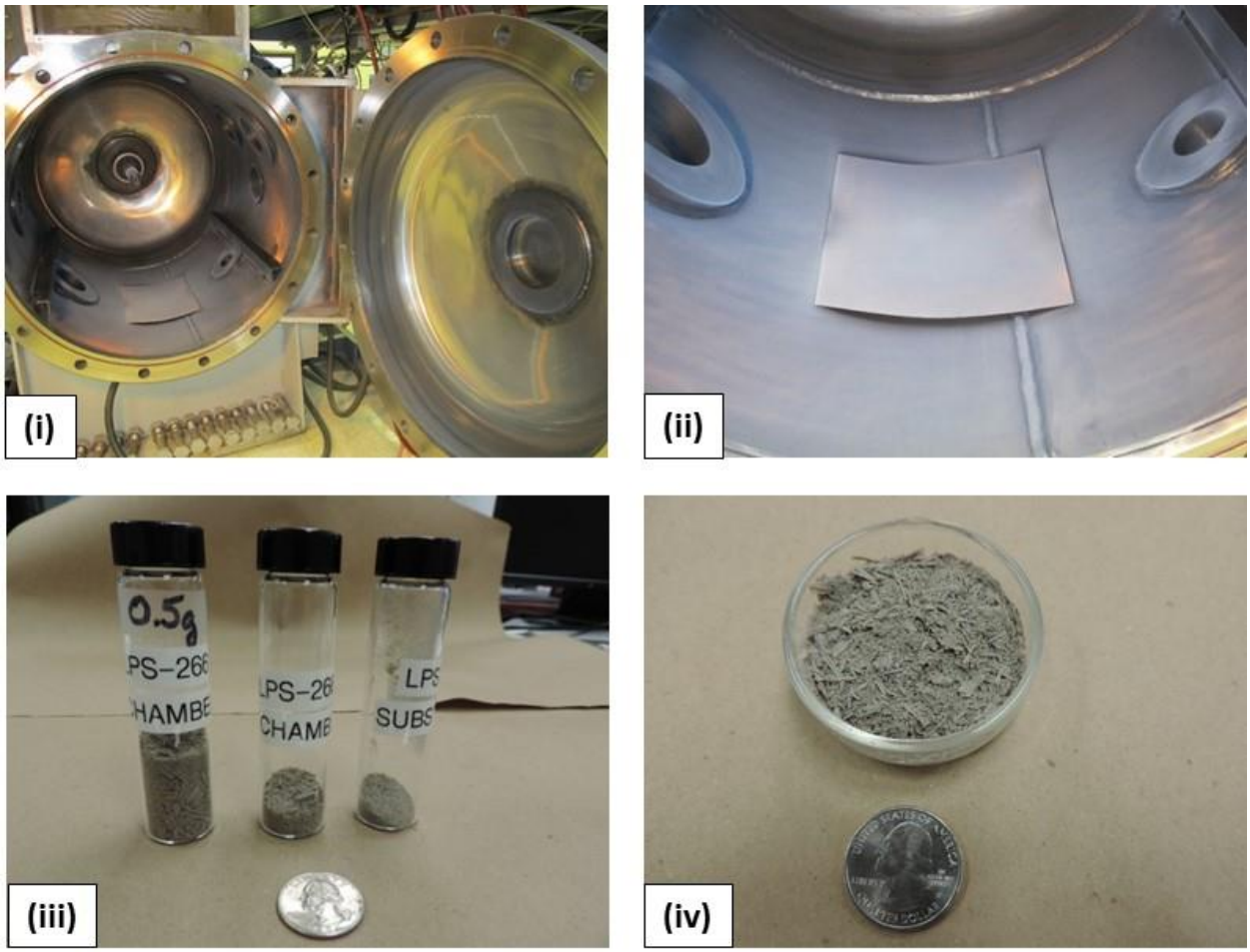

Figure 14. Material synthesized in the LaRC facility following a 15 min trial: (i) in the whole chamber; (ii) on a substrate foil on the chamber floor; (iii) following extraction from the substrate and the chamber walls; and (iv) very small product quantities, so far.

It is clear that clogging of the PF and the feed lines, as shown in figure 15, needs to be addressed. The configuration of the equipment does not lend itself to visual monitoring during a synthesis trial. The PF, Model 1264 manufactured by Praxair Surface Technologies is shown in figure 15(i). It is not rated for transport of nano-particulate or very low feed rates. The setup works well for metal deposition such as alloy Ti-6-4, which involves ~100 μm powder feedstock, and a ~30 g/min feed rate. Agglomeration of the powder is probably responsible for causing blockages, which may be occurring in the PF itself and/or the feed line leading to the RF torch, shown in figure 15(ii). The anti-static feed line and crude feeder vibrators which were installed proved ineffective. It is surmised that the target powder feed rate of 0.5 g/min for the 70 nm BN feedstock cannot be achieved with the current system. In lieu of procuring a new PF, the LaRC Acoustics Branch (Rizzi et al.) has been contracted to provide a near-term fix. Identifying the location of the "bottle neck" is the first objective. A transducer generating the appropriate amplitude and frequency, mounted to provide localized vibration appears to be a viable solution. The exit nozzle of the feeder, where the feed line is attached, is an obvious location to initiate studies.

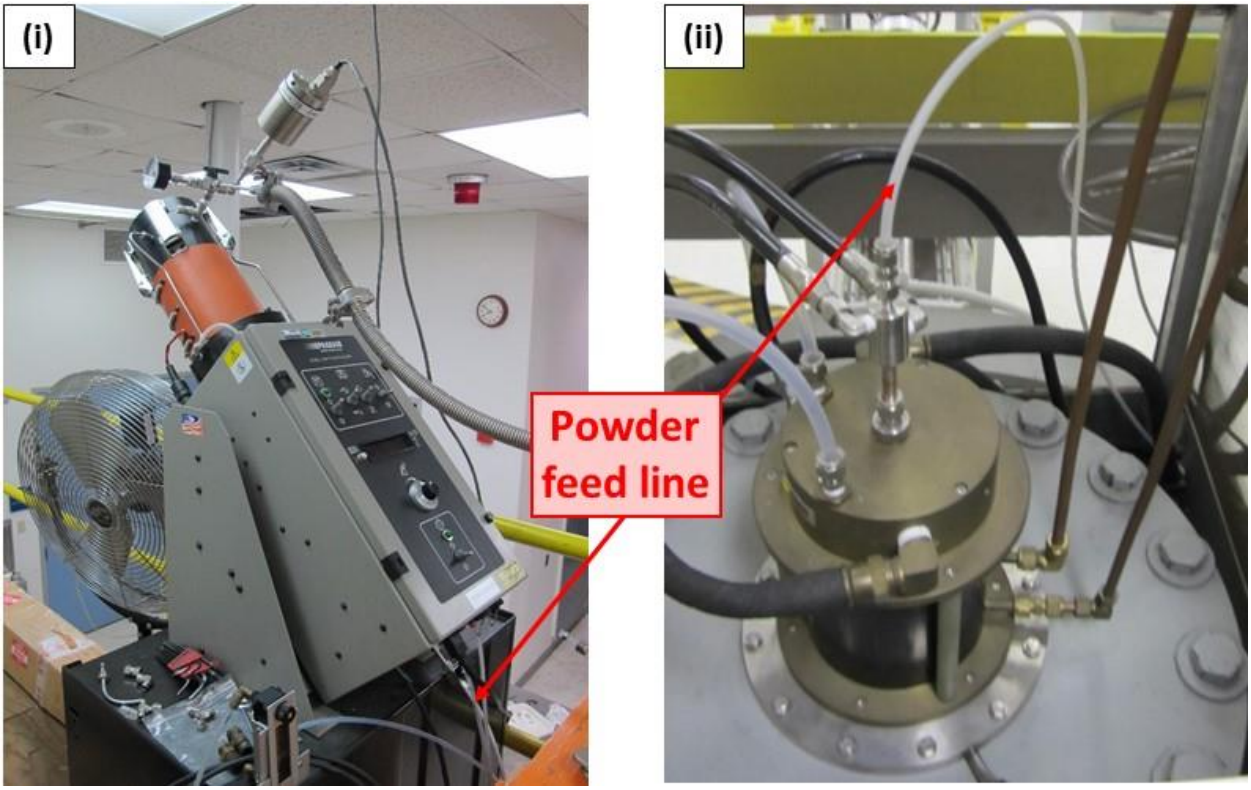

Figure 15.Diagnosing powder feeding issues within: (i) the Praxair Model 1264 powder feeder; and (ii) the injector probe on the Tekna torch. The suspected problematic locations where the feed line exits the powder feeder, and enters the injection probe, are highlighted.

NRC-C publications indicate that the feedstock is continuously fed by a KT20 twin-screw micro-feeder, manufactured by K-Tron, Inc., Sewell, NJ [ref. 18]. Most commercially-available PFs, including this one, are designed for atmospheric thermal spray of coarse metal, or ceramic, powders. Typical feedstock properties and requirements include high density, high flow-ability, low inter-particle cohesion, low bridging tendency, and high feed rates. The characteristics of 70 nm diameter h-BN powder are exactly the opposite, and the feed rate is low. The requirements are further complicated by the need to operate in a closed, low vacuum environment. Therefore, the original equipment, which was not rated for delivering nano-particulate, has been heavily modified by NRC-C. Evidently, it was a time-consuming challenge to achieve accurate and reproducible transport of feedstock at the prescribed rate [ref. 35]. Of significance to the LaRC effort, not only were equipment modifications required, but also engineering of the feedstock. NRC-C experimented with milling, sieving, and baking procedures to a variety of powders prior to loading in the feeder [ref. 14].

The smooth and reliable delivery of B or BN powder to the injector probe is critical in establishing steady state conditions within the reactor, and performing parametric studies to optimize the yield of BNNTs [ref. 35]. Efforts are currently underway to define the specifications for a replacement feeder system. Fluidized bed PFs, which are often specified for delivering non-conducting, ultrafine particulate, were explored as an option. However, the lack of accurate control at low feed rates eliminated them as a possibility. A vibrating PF which has

proved effective at delivering ~70 nm BN powder is manufactured by Tekna Plasma Systems, Inc., as shown in figure 16(i) [ref. 36]. Details of the construction and approximate dimensions are shown in the schematic in figure 16(ii). The PFR series feeder is rated for transporting 8 nm to 5 µm powders at rates of 0.5–40 rpm, graduated in increments of 0.1 rpm. It is probable that a similar device is being employed by Tekna for their NRC-C licensed BNNT production. The rotation speeds (rpm) quoted by the vendor need to be converted into mass feed rates (g/min) via customer calibration [ref. 36].

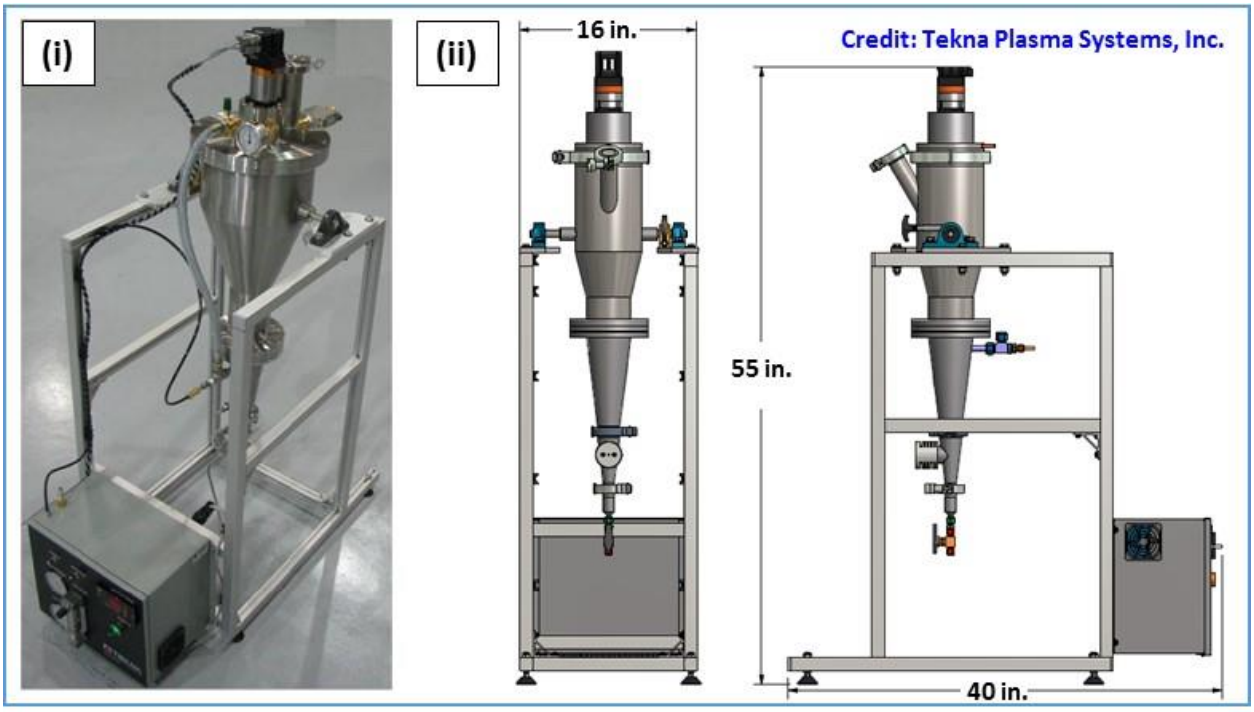

Figure 16. A vibrating powder feeder, PFR series manufactured by Tekna is compatible with feeding ultrafine powders at very low rates [ref. 36]: (i) image of device; and (ii) construction schematics. A similar system has successfully been used to transport 70 nm BN powder feedstock.

Another important way to improve the process yield is to quantify the plasma characteristics and correlate them with equipment settings. The large number of process variables listed in table 3 calls for statistically designed experimentation. However, the parametric limits have to be defined first for the effective application of such methodology. It is anticipated that the implementation of quantitative process diagnostics can aid in this regard. Delivery of the enthalpy probe system shown in figure 17, procured from Tekna Plasma Systems, Inc., is imminent [ref. 37]. The system measurements determine the specific enthalpy associated with a known amount of extracted gas. The composition, temperature, velocity, and density of the plasma gas mixture are then computed from the data gathered. Quantifying process conditions, as a function of position within the plasma plume, can then be related back to equipment settings. Subsequent correlation of thermal and compositional profiles with BNNT yield and aspect ratio

will be paramount during LaRC process development. Concurrent insertion of the data compiled into existing models will facilitate comprehension of the synthesis process [refs. 30 and 38].

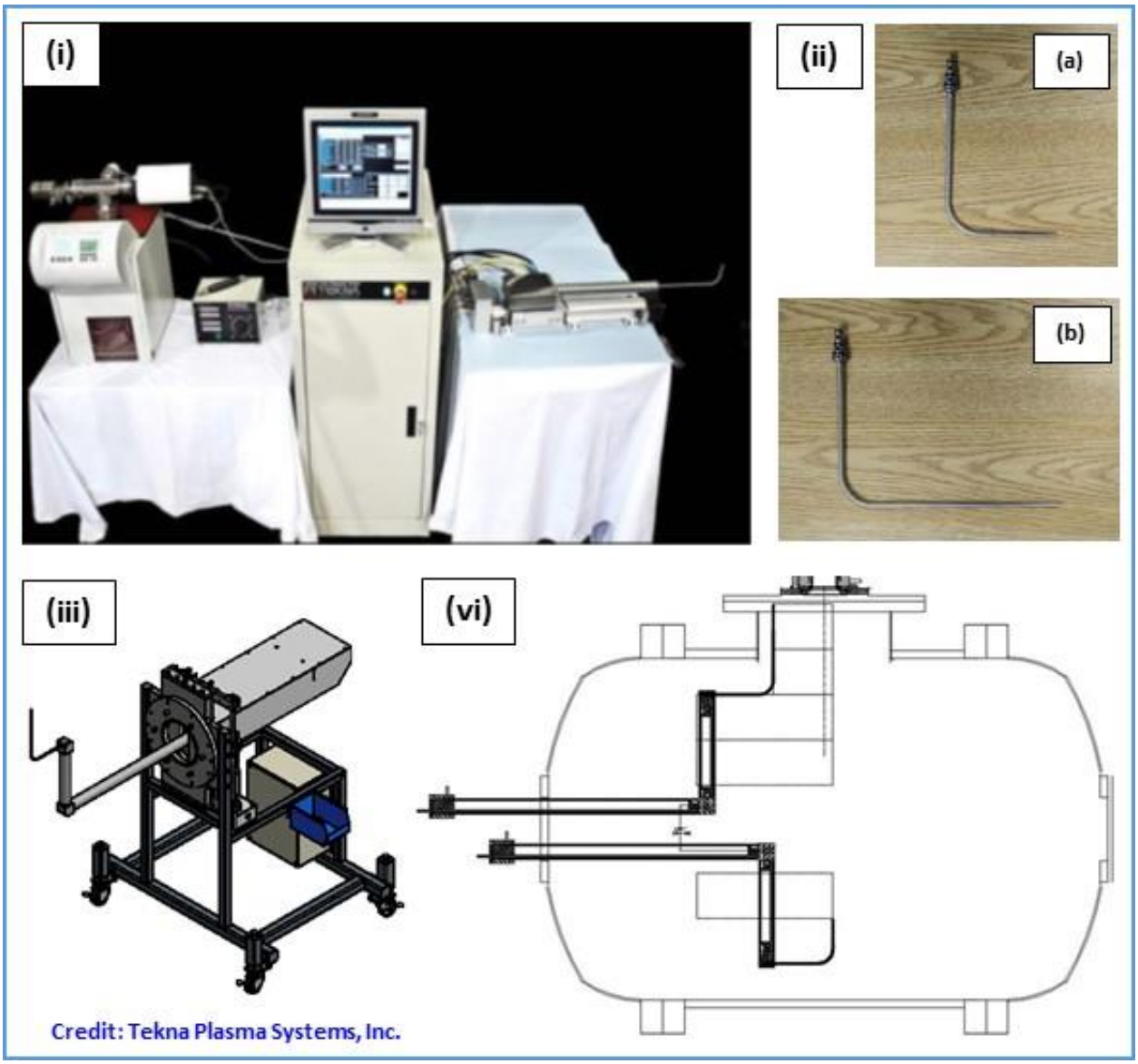

Figure 17. Procurement of a diagnostic enthalpy probe system, custom manufactured by Tekna [ref. 37]: (i) control console (center), probe assembly (right) and mass spectrometer (left); (ii) short (above) and long (below) options for probe installation; (iii) probe manipulator carriage schematic; and (iv) illustration of probe travel limits within the LaRC reaction chamber.

The image in figure 17(i) shows the control console, touch screen, enthalpy probe, and mass spectrometer. In contrast with other measuring devices, the operating temperature range of water-cooled enthalpy probes is greatly extended. For example, plume temperatures of ~6500 K in Ar/H_2 plasmas, and ~8000 K in Ar plasmas have been measured directly [ref. 11]. The images

in figure 17(ii) show the short, (a), and long, (b), enthalpy probe options for installation on the manipulation system. Shown schematically in figure 17(iii), the custom-designed probe manipulator will enable profiling of the whole reaction chamber. Mapping of the reactor will be performed during "dry runs" in order to establish equipment settings for BNNT synthesis. This is because the probe disrupts the plasma flow when inserted, and the tip is easily fouled by liquid or solid reactants [ref. 11]. Figure 17(iv) illustrates the motion limits of probe manipulation in the reactor. The assembly will be integrated through a large port on the end of the chamber, replacing the retractable target/substrate apparatus. The manipulator arm can be mounted in two positions and both the sub-assembly and probe can be rotated to provide maximum travel [ref. 37]. The easily-fouled assembly will be retracted during actual BNNT production operations.

3.2. Analysis

Becoming familiar with techniques compatible with analysis of BNNT materials was an integral part of this year's activities. The most commonly employed qualitative techniques are high resolution scanning electron microscopy (HRSEM) and Fourier transform infrared (FT-IR) spectroscopy. FT-IR techniques are used to obtain an absorption or emission IR spectrum (from a solid, liquid, or gas) over a wide range of wavelengths using a FT to convert the raw data [ref. 39]. The peaks on a spectrum are indicative of different atomic bonds and how the components of a particular sample react to light as a function of wavelength. Both methods allow ready comparisons between the characteristics of the powder feedstock, as-synthesized product, purified materials, and reaction by-products. A simple purification technique, adopted from work by Chen et al. [ref. 40], is routinely used by NRC-C to isolate BNNTs. The data accrued from purified BNNT materials tend to be easier to interpret, providing the yield is sufficient.

Figure 18 shows FT-IR spectroscopy results for RF synthesized BNNT materials. Figure 18(i) shows the LaRC preliminary data (in absorbance mode), and figure 18(ii) shows the NRC-C data (in transmittance mode) [ref. 27]. The NRC-C data are presented such that the signatures of the feedstock and the typical synthesis products are separated. FT-IR results can be presented in several different formats, but the prime peaks related to B-N bonds remain at the same wavenumbers, i.e., 815 and 1369 cm^{-1}. The LaRC data (blue line) are difficult to interpret based on the NIST standard (red line), which is also plotted [ref. 41]. Comparing with the NRC-C data, the presence of BNNTs in the as-synthesized product may be masked by an excess of reaction by-product. This generates many spurious peaks, which are mostly associated with components containing –H bonds (highlighted).

The HRSEM images in figure 19 compare the results from RF plasma synthesis trials performed at LaRC and NRC-C. Figure 19(i) shows the starting BN feedstock for the LaRC trials, with a nominal particle size of 70 nm. Figure 19(ii) shows the results from LPS 266, and reveals the product characteristics typical of the current trials. Figure 19(iii) shows the synthesized product from an early NRC-C trial for comparison. H_2 was not included in the plasma forming gas mixture and analysis revealed the presence of no BNNTs [ref. 14]. Comparing figure 19(ii) and (iii) suggests that the features of the two products are very similar. In conjunction with the FT-IR data, there is no evidence to suggest that BNNTs have been generated during the LaRC trials to-date. However, the results are encouraging, and also highlight the need for purification to eliminate reaction by-products for future analyses.

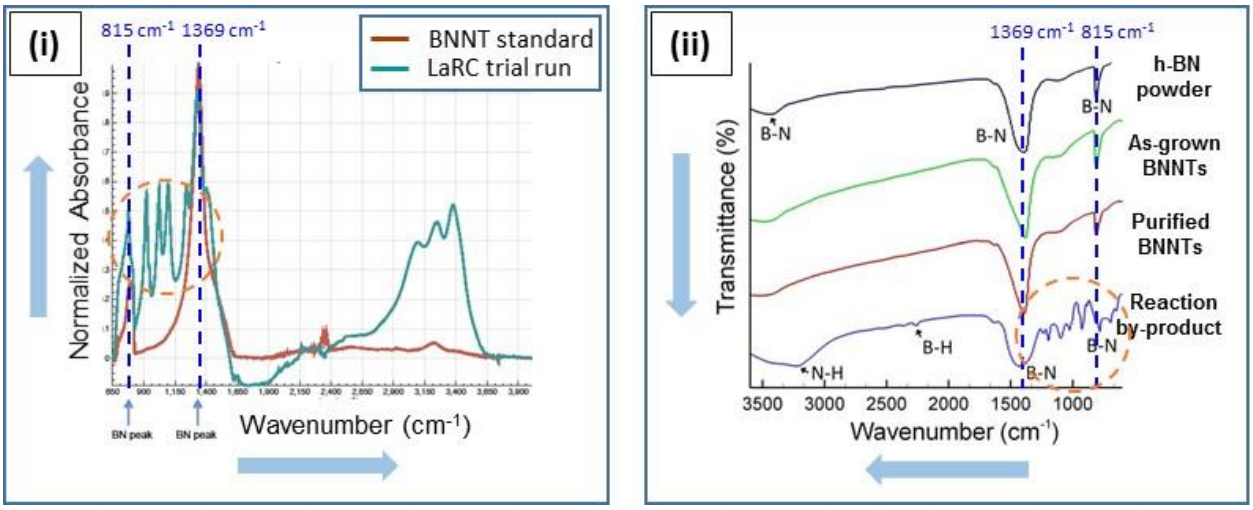

Figure 18. FT-IR spectroscopy results for BNNT synthesis products: (i) LaRC preliminary data (in absorbance mode), compared with BNNT standard signature [ref. 41]; and (ii) NRC-C data (in transmittance mode), presented so that the traces for the feedstock and various synthesis products are separated [ref. 27].

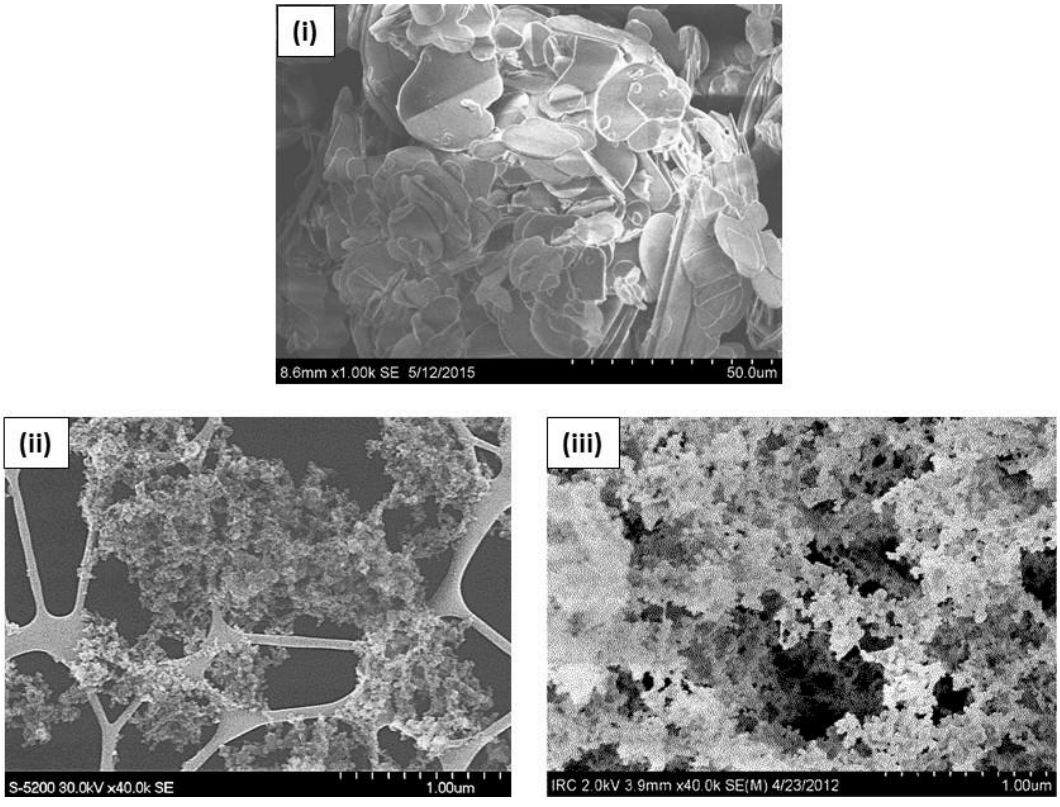

Figure 19. HRSEM images: (i) starting BN feedstock at low magnification; (ii) LPS 266 product on a carbon grid; and (iii) NRC-C product from an early synthesis trial using no H_2 in the plasma gas [ref. 14]. A comparison of (ii) and (iii) suggests that BNNTs were not formed during the current LaRC trials.

In the event that sufficient product is generated, purification of the as-synthesized material will lead to more thorough HRSEM and FT-IR analyses. BNNTs tend to be much more thermally stable than the reaction by-products [refs. 27 and 28]. The post-synthesis protocol developed for extraction of BNNTs via thermal treatment and dissolution of reaction by-products is outlined in figure 20. Thermo-gravimetric analysis (TGA) has revealed that pure BNNTs undergo zero weight gain to temperatures in excess of 1173 K (figure 20(i)) [ref. 27]. In the as-synthesized condition, both the fibril- and cloth-like BNNT materials begin to gain weight at ~873 K, figure 20(ii) [ref. 28]. The reason for the weight gain was established by Chen et al. [ref. 40], whose purification protocol was adopted by NRC-C. The formation of boron oxide (B_2O_3), resulting from oxidation of amorphous B and BN-containing particles, causes the increase. Thus, an oxidizing heat treatment renders the by-products water soluble, and a simple rinse suffices for removal. The earlier NRC-C publications indicate baking in air at 698 K for 3 days [ref. 27]. It was recognized that this was a mild oxidation condition for B, and it was intentionally used to minimize BNNT damage. The later NRC-C patent suggests baking in air at a more aggressive 923–1073 K for an unspecified duration [ref. 14]. The Chen work suggests 1073 K for 1 hour, followed by hot water washing and drying at 373 K is effective [ref. 40]. This will be the protocol adopted for the ongoing LaRC effort, since it has been shown to work well. As progress is made, this might also prove to be a quick and easy method for assessing the percent yield of BNNTs following individual synthesis trials.

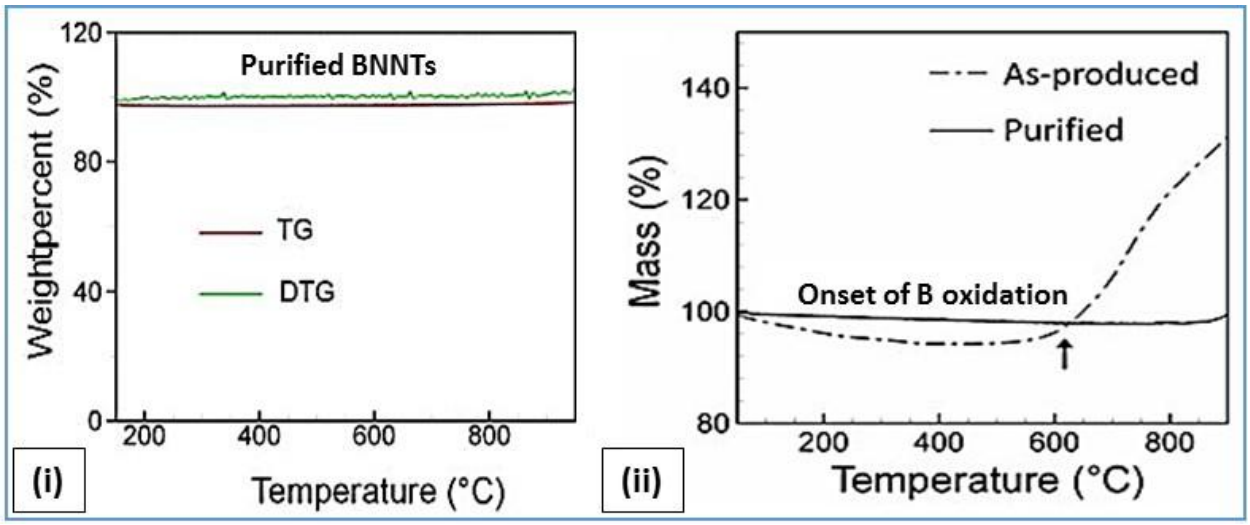

Figure 20. NRC-C data demonstrating the thermal stability of BNNT materials via TGA results: (i) purified BNNT material using established protocol [ref. 27]; and (ii) comparison of as-synthesized and purified BNNT materials [ref. 28]. Any weight gain is primarily due to oxidation of untransformed B particles.

3.3. Collection

Another important objective of the LaRC effort is the assessment and implementation of in-line, dry separation techniques for the collection of "fluffy" BNNTs. Operational safety was a primary consideration in all LaRC RFPS activities [ref. 42]. The self-imposed mandate was zero tolerance for airborne BNNT-containing materials. The adoption of dry methods for

purification/collection of bulk BNNT materials could be very beneficial. Further, if continuous, in-flight classification/fractionation techniques can be developed, then post-synthesis processing could be greatly simplified. It may even be possible to exploit the unique configuration of the LaRC RFPS facility to utilize a binning process for sorting by aspect ratio.

Both of the incumbent practices (NRC-C and UC-B) tend to produce tangled masses of fibril-, cloth-, and cotton candy-like materials within the reactor or filtration device [refs. 12, 15, and 18]. Experience also indicates that the subsequent use of organic solvents for secondary sorting of BNNTs leads to irreversible contamination [ref. 35]. NRC-C recognizes that secondary, wet separation techniques are an issue and is exploring in-situ BNNT handling methods. Figure 21(i) illustrates a prototype in-line, dry separation collection system which has been developed [ref. 28]. As shown in the inset, the device is rudimentary and consists of a rotating "cold finger" mounted within the exhaust pipe. Figure 21(ii) shows that the cylindrical drum accumulates BNNT material as it exits the synthesis reactor. It is touted as being used for "direct fabrication of BNNT sheets," as shown in figure 21(iii). Such a process might be scalable, but it is confined to batch processing and has very specific application.

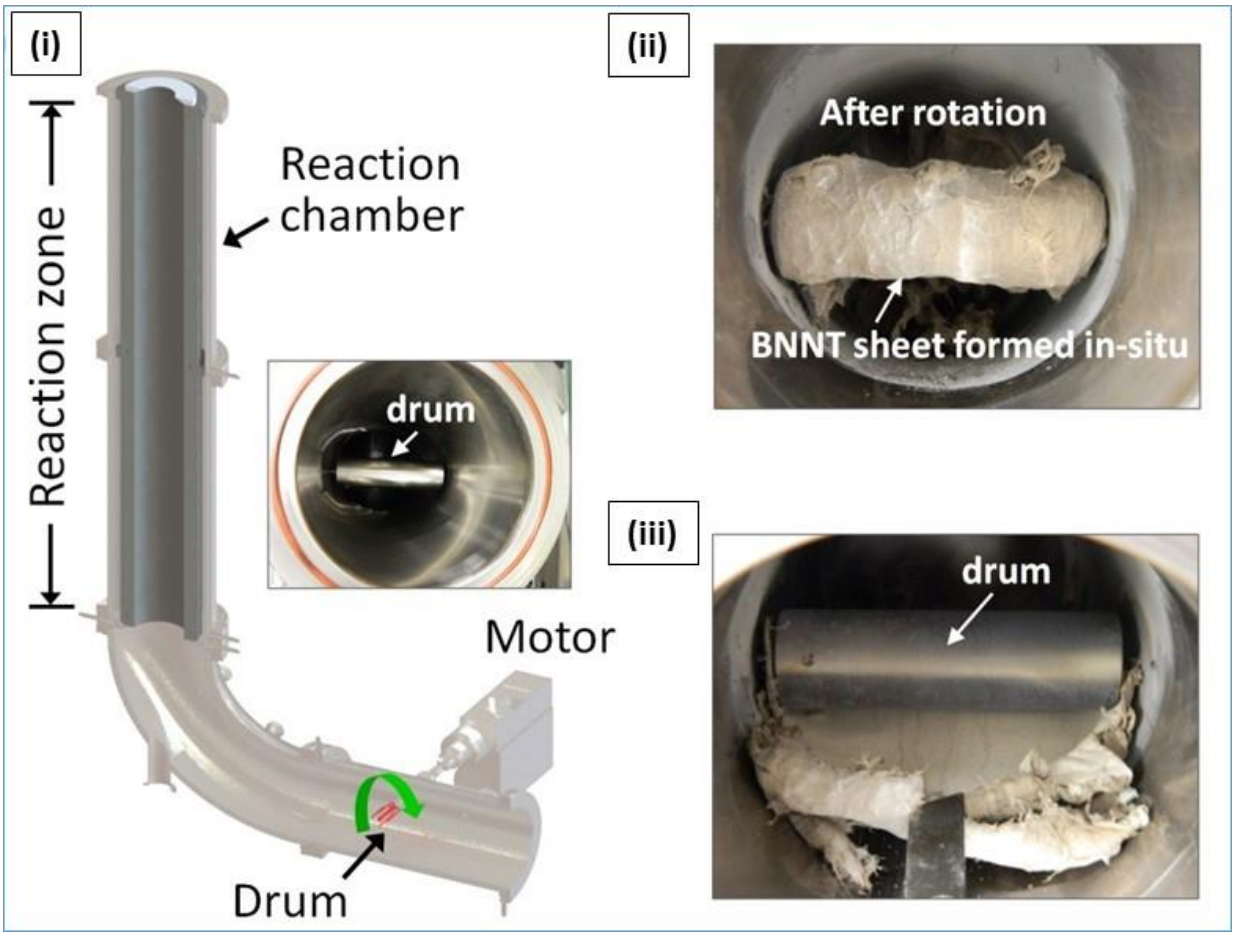

Figure 21. A prototype in-line, dry separation system developed by NRC-C [ref. 28]: (i) a small, rotating drum mounted in the exhaust near the reactor exit; (ii) synthesis product collected on the drum; and (iii) peeling of BNNT sheet material from the drum.

In the CNT production industry, collection vessels which employ centrifugal force to progressively separate the product contained in effluent gases have long been touted [ref. 43]. Cyclonic separators are alluded to in many CNT synthesis patents, but equipment specifics tend to be sparse. Figure 22 shows an example of the setup developed by the Honda Motor Co. (Japan) [ref. 44]. Figure 22(i) shows banks of collection vessels, which employ centrifugal force to isolate the reaction product, and sequentially sort the particulate by weight. Figure 22(ii) illustrates the dimensions pertaining to a single cyclone that are critical to performance. The efficiency of cyclone separators in removing particles of varying size depends on the diameters of the (1) cyclone, D_1, (2) particulate outlet, D_2, (3) gas inlet, D_3, and (4) gas outlet, D_4 [ref. 45]. The configuration of each cyclone in the series needs to be individually optimized for the whole system to be effective.

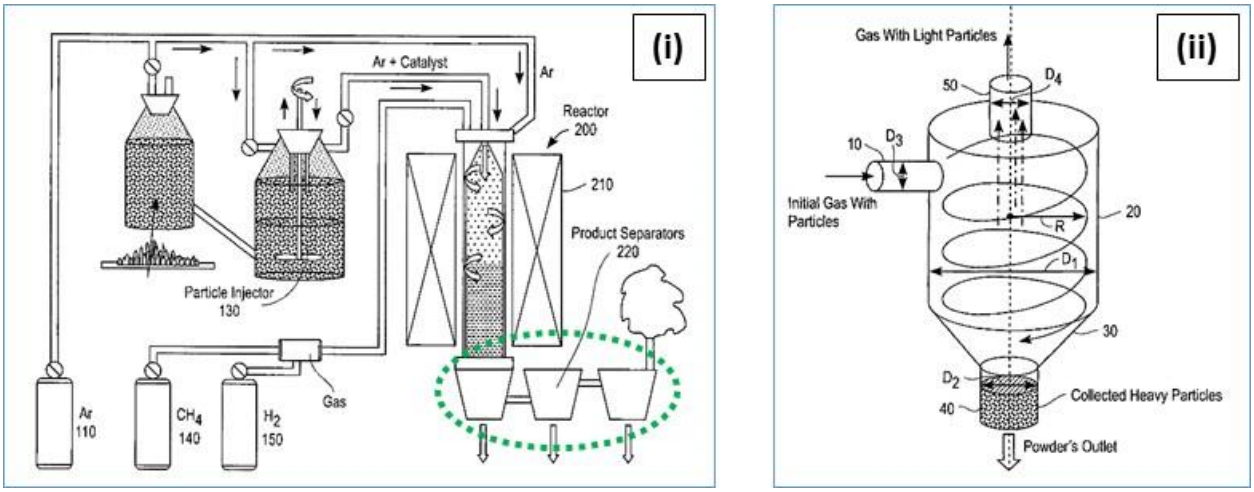

Figure 22. In-line, dry separators used in commercial CNT production: (i) a series of cyclonic devices (highlighted) with binning capability; and (ii) dimensions critical to individual cyclone performance, i.e., collection efficiency for a specified powder outlet size range [ref. 44].

Cyclone technology is mature for both emission control and product recovery on multiple scales [ref. 45]. The examples shown in figure 23 are designed and manufactured by Advanced Cyclone Systems, Inc, Porto, Portugal, a recognized industry leader [ref. 46]. Large units, as shown in figure 23(i), have been developed for progressively more sophisticated pollution control, including coping with high temperature flue gases. In the majority of applications, the particles extracted from the gas flow are discarded, and only recently has close attention been devoted to recovery of very fine particles. An exception is the pharmaceutical industry, where collection of every gram of product tends to be prized [ref. 47]. As shown in figure 23(ii), small units have been developed for ultraclean, highly efficient recovery of products, which are of the most relevance to BNNT synthesis applications.

An extensive literature search focusing on gas-solid separation technology was conducted this year. Accepting that the ultimate goal is integrated collection of product at operating temperatures, an immediate solution for near-term handling of product was required. As a consequence, specifications for collection at ambient temperature were established and

commercial vendors were identified. Progress has advanced along two fronts for near-term and future application;

- A conventional cyclone/pneumatic vacuum system for product collection at ambient temperature was designed and installed.
- An electro-static cyclone system for product collection (fractionation) at operating temperatures was down-selected.

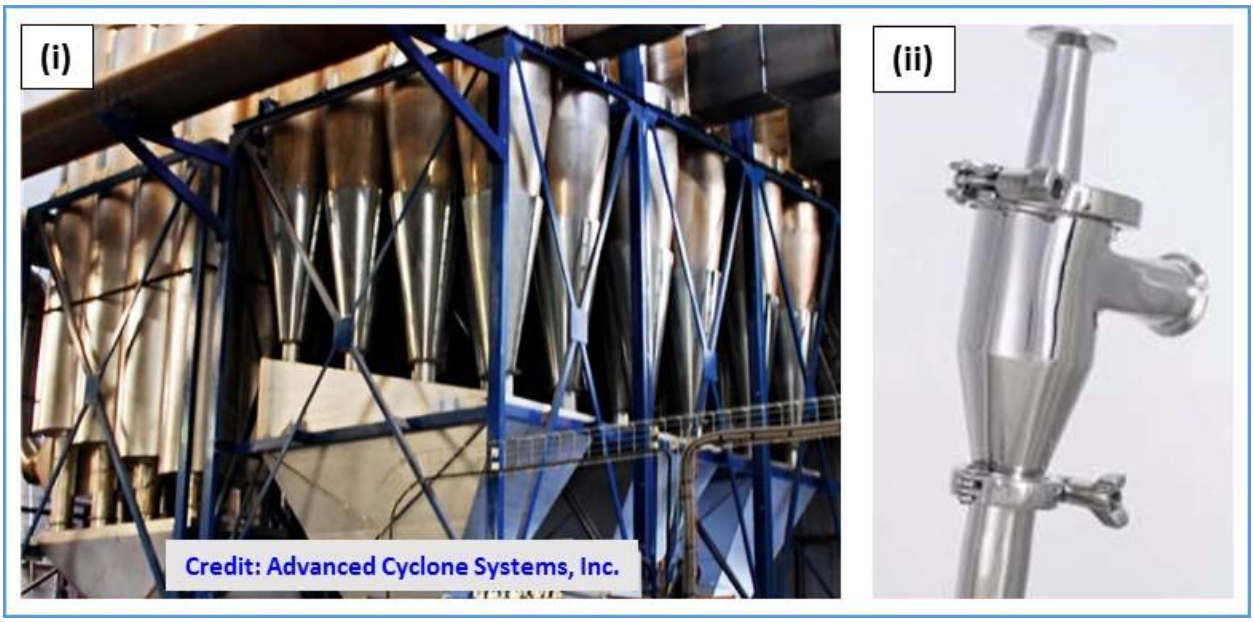

Figure 23. Application spectrum of cyclone technology for nano-particulate collection by ACS, Inc.: (i) emission control—large, multiple units designed for high volume and/or high temperatures [ref. 46]; and (ii) product recovery—smaller, individual units designed for efficiency and cleanliness [ref. 47].

As shown in figure 24(i) and (ii), the ambient temperature system procured comprises two devices connected in series. Figure 24(iii) shows the high efficiency cyclone pre-separator with direct bagging system, manufactured by Ruwac USA, Holyoke, MA. The critical dimensions of Model 9949-E, which is rated at 2830–7080 slpm, comprise cyclone diameter = 20 cm, inlet diameter = 5 cm, and outlet diameter = 5 cm. The cyclone pre-separator is driven by a pneumatic wet/dry vacuum system, manufactured by Tornado Industries, West Chicago, IL, shown in figure 24(iv). It was recognized that an electric pump might be a source of ignition for ultrafine particulate. The Dual Air Jumbo (Model 95962) system is rated at 9630 slpm and 4530 slpm at the orifices. This is operated in wet mode, i.e., the process effluent passes through de-ionized water in the containment vessel. This guarantees that no highly mobile nano-particles will escape to atmosphere. Although this is far from satisfactory from the perspective of dry processing, the use of organic solvents is avoided.

Figure 24. Ruwac cyclone and Tornado pneumatic vacuum system connected in series for dry collection at room temperature: (i) side view of setup; (ii) overhead view of setup; (iii) exhaust exits chamber and enters cyclone; and (iv) exhaust exits cyclone and enters twin pneumatic suction pumps.

The shortcomings of conventional cyclones for collecting nano-particulate stem from the lower limit of the collection range. Purely centrifugal-type separators are most efficient in the 0.5–1000 μm range [ref. 48]. Cyclone separators tend to suffer from poor collection efficiency when coping with product consisting primarily of sub-micron particles. In contrast, electrostatic-type separators are effective in the 1 nm–10 μm range [ref. 48]. Standard electrostatic precipitators fall into three broad categories: charged plates, wires, or drums [ref. 49]. Applications primarily involve the separation of conducting and non-conducting particles [ref. 50]. Specialized systems have also been developed for dealing with large quantities of non-conductive particulate [ref. 51]. From this perspective, wire-in-pipe systems hold the most promise for small scale, continuous processing. Hybrid systems are also evolving, which include electro- or electrostatic cyclones, and electrostatically-assisted or -enhanced cyclonic systems [ref. 45]. Selecting from among commercially available, hybrid cyclonic/electrostatic systems seemed prudent for the operating temperature system. One such system is already being employed in the pharmaceutical industry for efficient collection of nano-powders. As shown in figure 25, Physical Sciences Incorporated, Andover, MA, has already demonstrated that a Recylone EH system procured from ACS, Inc. (Portugal) can collect 90% of particles in the 20–30 nm range [ref. 52].

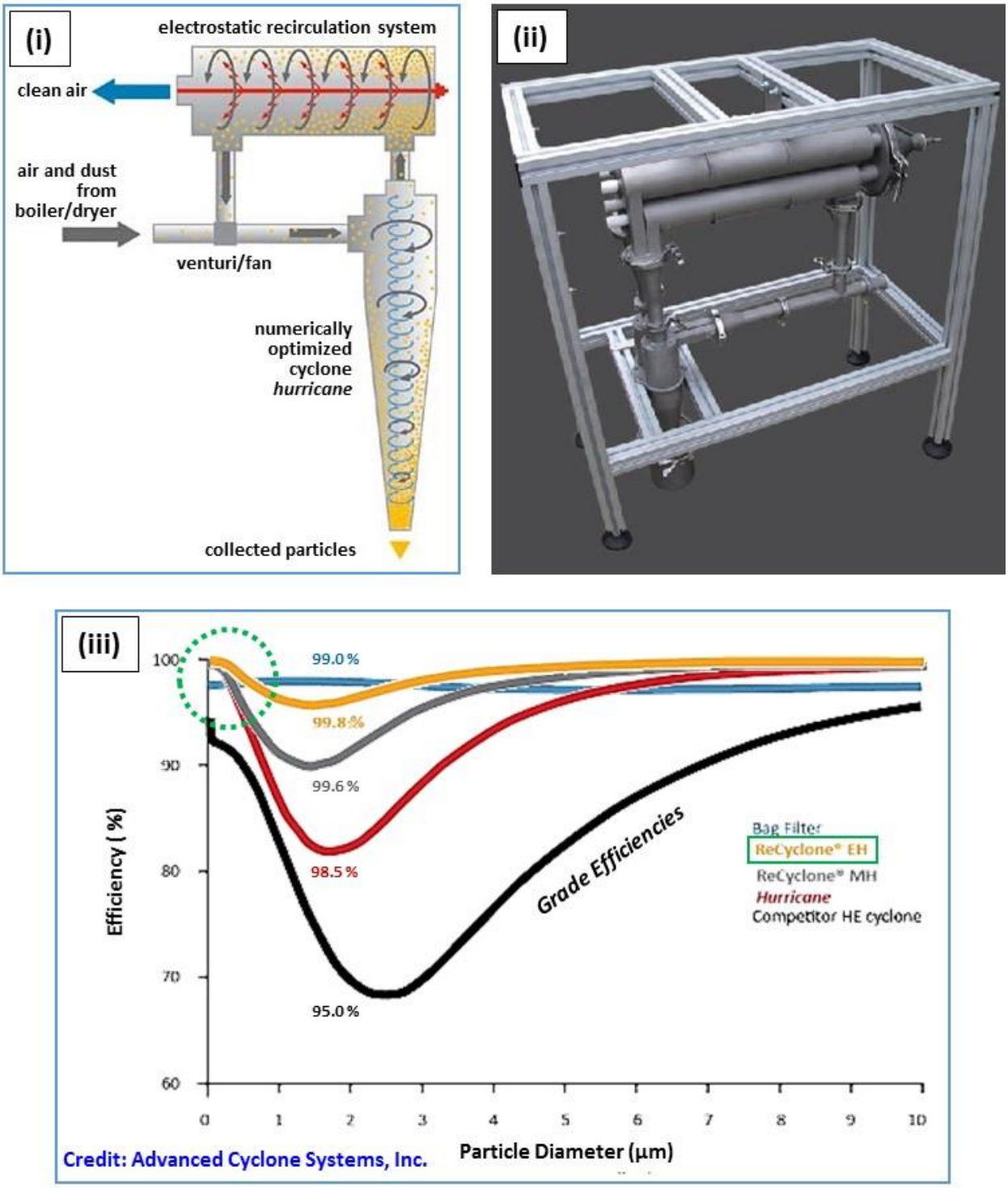

Figure 25. Recyclone EH, manufactured by Advanced Cyclone Systems, Inc., consists of a customized cyclone assisted by an electrostatic recirculator: (i) configuration of the apparatus [ref. 46]; (ii) image of a system installed at Physical Sciences Inc. [ref. 47]; and (iii), collection efficiency of a system (superior performance in the nanometer range highlighted) [ref. 47].

As illustrated in figure 25(i), the Recylone EH concept involves a wire-in-pipe electrostatic separator that is mounted atop a conventional cyclone [ref. 47]. Process effluent is first treated by a conventional cyclone, and then by an electrostatic device, before being returned to the cyclone for further treatment. An isolated cycle through the system might be envisioned as follows. Particulate that is too fine ($d < 0.5$ μm) to be removed from the inlet gas flow during the first pass is recycled through the separator. The partially-cleansed gas travels through the electrostatic recirculator in a helical pattern. The applied field causes the particles to agglomerate into bundles which are big enough to be removed by the cyclone on the second pass. The 1 m long by 1 m high chassis containing the apparatus installed at Physical Sciences Inc. is shown in figure 25(ii) [ref. 47]. Numerical optimization based on customer input dictated that a dual system was fabricated to satisfy the requirements. It is considered a laboratory-scale system and consists of a bank of four electrostatic recirculators plumbed with twin cyclones.

The performance of the different system configurations offered by ACS, Inc. is shown in figure 25(iii) [ref. 47]. Attention is drawn to the yellow line which represents the Recyclone EH. This system exhibits the top performance over all particle sizes and is clearly the best option for a collection of nano-sized particulate. Discussions with ACS, Inc. suggest that a system very similar to this, custom-designed to operate at 200°C with a gas flow rate of 250 slpm, would be compatible with the LaRC RFPS facility [ref. 53]. The concept of using such a system for fractionation of BNNT materials was raised with the vendor. The potential for the recirculated stream(s) to be redirected to separate collectors was introduced for future consideration.

4. Concluding Remarks

- The project goal is to produce quality (based on purity and aspect ratio) BNNTs in quantities sufficient to allow the potential performance benefits of BNNT-reinforced metallic and/or ceramic matrix composites to be evaluated.
- The pros and cons of high temperature processes for BNNT synthesis were identified. Laser ablation methods can produce high quality BNNTs, but at low production rates, so the focus was on RF plasma-based systems.
- RF processing depends on plasma torch capability, plume shape and characteristics, chamber size, and geometry. Experimental parameters tend to be equipment-specific and include reaction gas composition, chamber pressure, BNNT collection process, and purification methods.
- A manageable number of experiments is required, so a diagnostic enthalpy probe system has been procured. The enthalpy probe will allow characterization of plasma plume properties and quantitative mapping of the entire reaction zone. This will permit the science of the synthesis process to be better understood. Armed with this additional knowledge, optimization of BNNT quality and yield will be more readily achievable.
- Incumbent BNNT purification methods have been analyzed and evaluated. Wet methods will be avoided due to negative effect of solvents on products. Current dry methods are rudimentary and provide no separation of product based on purity or aspect ratio.
- A pneumatic-powered cyclone system has been installed that performs at room temperature, thereby providing a safe, near-term collection capability. An electro-static cyclone system has been down-selected for product collection/fractionation at operating temperatures. It is anticipated that this will provide an avenue for an in-line, continuous production process.
- Six BNNT synthesis runs have been performed and measureable quantities of BNNT-containing material have yet to be produced.
- The inadequate performance of the current powder feeder was identified as a significant problem. The system has only been used previously to deliver heavy and relatively coarse metallic powders to the injection probe at much higher rates. It is surmised that this feeder is incapable of accurately feeding lightweight, ultrafine B or BN powders at prescribed lower rates. A commercially-available powder feeder capable of properly feeding B powders has been identified and will be procured to resolve this issue.
- All current problems have been identified and addressed. Operating conditions have been bracketed to facilitate ongoing BNNT synthesis trials.

5. Acknowledgements

The authors are grateful to the following people at Langley Research Center who provided technical assistance on this project (listed in alphabetical order):

- James Baughman: Analytical Mechanics Associates, Inc., D307
- Harold Claytor: Analytical Mechanics Associates, Inc., D307
- Peter Messick: Analytical Mechanics Associates, Inc., D307
- Cheol Park: NASA, Advanced Materials and Processing Branch, D307
- Stephen Rizzi: NASA, Aeroacoustics Branch, D314
- Louis Simmons: NASA, Advanced Fabrication Processes Section, D212B
- Matthew Stearman: Science & Technology, Corp., D213
- Wesley Tayon: NASA, Advanced Materials and Processing Branch, D307
- Travis Turner: NASA, Aeroacoustics Branch, D314
- Stewart Walker: Analytical Mechanics Associates, Inc., D307

6. References

1. C.E. Harris, M.J. Shuart, and H.R. Gray, "A survey of emerging materials for revolutionary aerospace vehicle structures and propulsion systems," NASA/TM-2002-211664, Langley Research Center, Hampton, VA, May, 2002.
2. C.T. Kingston, "Large-scale synthesis of few-walled small diameter boron nitride nanotubes (sub-10 nm) by an induction thermal plasma," NRC-Canada, Presentation at NT13, 14th International Conference on the Science and Applications of Nanotubes, Aalto University, Finland, June 28, 2013.
3. K.J. Koziol, J. Vilatela, A. Moisala, M. Motta, P. Cunniff, M. Sennett, and A. Windle, "High-performance carbon nanotube fiber," Science, vol. 318, no. 5858, pp.1892–1895, 2007.
4. X. Wei, M.S. Wang, Y. Bando, and D. Golberg, "Tensile tests on individual multi-walled boron nitride nanotubes," Adv. Mater., vol. 22, no. 43, pp. 4895–4899, 2010.
5. B.G. Demczyk, Y.M. Yang, J. Cumings, M. Hetman, W. Han, A. Zettl, and R.O. Ritchie, "Direct measurement of the tensile strength and elastic modulus of multiwalled carbon nanotube," Mater. Sci. & Eng. Vol. A334, nos. 1–2, pp. 173–178, 2002.
6. C.Y. Zhi, Y. Bando, C.C. Tang, and D. Golberg, "Boron nitride nanotubes," Mat. Sci. Eng. R, vol. 70, nos. 3–6, pp. 92–111, 2010.
7. M.L. Cohen and A. Zettl, "The physics of boron nitride nanotubes," Physics Today, pp. 34–38, November, 2010.
8. G. Sauti, C. Park, J.H. Kang, J.W. Kim, J.S. Harrison, M.W. Smith, K.C. Jordan, S.E. Lowther, P.T. Lillehei, S.A. Thibeault, "Boron nitride and boron nitride nanotube materials for radiation shielding," Langley Research Center, Hampton, VA, US Patent Application #2013/0119316 A1, May 16, 2013.
9. N.G. Chopra, R.J. Luyken, M.L. Cohen, and A. Zettl, "Boron nitride nanotubes," Science Magazine, vol. 269, pp. 966–967, August, 1995.
10. M.W. Smith, K.C. Jordan, C. Park, J.W. Kim, P.T. Lillehei, R. Crooks, and J.S. Harrison, "Very long single- and few-walled boron nitride nanotubes via the pressurized vapor/condenser method," Nanotechnology, vol. 20, no. 50, 505604, 6 pp., 2009.
11. P. Fauchais, "Understanding plasma spraying," J. Phys. D: Appl. Phys., vol. 37, pp. R86–R108, 2004.
12. A. Fathalizadeh, T. Pham, W. Mickelson, and A. Zettl, "Scaled synthesis of boron nitride nanotubes, nanoribbons, and nanococoons using direct feedstock injection into an extended-pressure, inductively-coupled thermal plasma," ACS Nano Lett., vol. 14, no. 8, pp. 4881–4886, 2014.
13. A.K. Zettl, "Method and device to synthesize boron nitride nanotubes and related nanoparticles," University of California, Oakland, CA, US Patent Application # 2013/0064750, March 14, 2013.

14. K.S. Kim, C.T. Kingston, and B. Simard, “Boron nitride nanotubes and process for production thereof,” NRC-Canada, Canadian Patent Application # CA 2877060 A1, October 23, 2014.

15. K.S. Kim, M.B. Jakubinek, Y. Martinez-Rubi, B. Ashrafi, J. Guan, K. O’Neill, M. Plunkett, A. Hrdina, S. Lin, S. Denommee, C.T. Kingston, and B. Simard, “Polymer nanocomposites from free-standing, macroscopic boron nitride nanotube assemblies,” RSC Advances, vol. 5, no. 51, pp. 41186–41192, 2015.

16. K.S. Kim, A. Moradian, J. Mostaghimi, Y. Alinejad, A. Shahverdi, B. Simard, and G. Soucy, “Synthesis of single-walled carbon nanotubes by induction thermal plasma," Nano Res, vol. 2, no. 10, pp. 800–817, 2009.

17. B. Simard, C.T. Kingston, S. Denommee, G. Soucy, and G. Cota-Sanchez, “Method and apparatus for the continuous production and functionalization of single-walled carbon nanotubes using high frequency plasma torch,” US Patent # 8,834,827, National Research Council, Ontario, Canada, September 16, 2014.

18. K.S. Kim, C.T. Kingston, A. Hrdina, M.B. Jakubinek, J. Guan, M. Plunkett, and B. Simard, “Hydrogen-catalyzed, pilot-scale production of small-diameter boron nitride nanotubes and their macroscopic assemblies,” ACS Nano, vol. 8, no. 6, pp. 6211–6220, 2014.

19. Y-T.R. Lau, M. Yamaguchi, X. Li, Y. Bando, D. Golberg, and F.M. Winnik, “Length fractionation of boron nitride nanotubes using creamed oil-in-water emulsions,” Langmuir, ACS Publications, vol. 30, pp. 1735–40, 2014.

20. H.W. Hao, K.K. Ting, L.J. Horng, and S.Y. Ting, “Investigation of nonwoven carding process with the application of static electricity to various fibres and process parameters,” J. Fibres & Textiles in Eastern Europe, vol. 15, no. 1, pp. 76–81, 2007.

21. Thomson Reuters; http://www.reuters.com/article/idUSnMKWFNJ1Ja+1fa+MKW20140827.

22. Tekna Plasma Systems, Inc.; http://tekna.com/tekna-launches-a-revolutionary-material-on-the-market-boron-nitride-nanotubes/.

23. R. Dolbec, M. Boulos, E. Bouchard, and N. Kuppuswamy, “Nanopowders synthesis at industrial-scale production using the inductively-coupled plasma technology,” Int. Conf. Advanced Nanomaterials and Emerging Engineering Technologies, IEEE, New Dehli, India, pp. 21–24, July, 2013.

24. M.I. Boulos, N. Dignard, A. Auger, J. Jurewicz, and S. Thelland, “High performance induction plasma torch,” Tekna Plasma Systems, Inc., Sherbrooke, Canada, US Patent Application # 2012/0261390, October 18, 2012.

25. M.I. Boulos, “New frontiers in thermal plasmas from space to nanomaterials,” Nuclear Eng. Technol., vol. 44, no. 1, pp. 1–8, 2012.

26. S.A. Esfarjani, S.B. Dworkin, J. Mostaghimi, K.S. Kim, C.T. Kingston, B. Simard, and G. Soucy, “Detailed numerical simulation of single-walled carbon nanotube synthesis in a radio-frequency induction thermal plasma system,” HTPP-12, IOP Publishing, J. Phys.: Conference series, vol. 406, 012011, 10 pp., 2012.

27. K.S. Kim, C.T. Kingston, A. Hrdina, M.B. Jakubinek, J. Guan, M. Plunkett, and B. Simard, "Hydrogen-catalyzed, pilot-scale production of small-diameter boron nitride nanotubes and their macroscopic assemblies," ACS Nano, vol. 8, no. 6, Supporting information, Published online May 7, 2014, http://pubs.acs.org/doi/suppl/10.1021/nn501661p/suppl_file/nn501661p_si_001.pdf.

28. K.S. Kim, M.B. Jakubinek, Y. Martinez-Rubi, B. Ashrafi, J. Guan, K. O'Neill, M. Plunkett, A. Hrdina, S. Lin, S. Denommee, C.T. Kingston, and B. Simard, "Polymer nanocomposites from free-standing, macroscopic boron nitride nanotube assemblies," RSC Advances, vol. 5, no. 51, Electronic supplementary information, Published online April 30, 2015, http://www.rsc.org/suppdata/c5/ra/c5ra02988k/c5ra02988k1.pdf.

29. "Boron," *Wikipedia, The Free Encyclopedia*, last modified October 31, 2015, https://en.wikipedia.org/wiki/Boron, Accessed November 4, 2015.

30. J. Guo, X. Fan, R. Dolbec, S. Xue, J. Jurewicz, and M. Boulos, "Development of nanopowder synthesis using induction plasma," Plasma Science & Technology, vol. 12, no. 2, pp. 188–199, 2010.

31. R. Arenal, O. Stephan, J.-L. Cochon, and A. Loiseau, "Root-growth mechanism for single-walled boron nitride nanotubes in laser vaporization technique," J. Am. Chem. Soc., vol. 129, pp. 16183–16189, 2007.

32. "Boron nitride," *Wikipedia, The Free Encyclopedia*, last modified November 11, 2015, https://en.wikipedia.org/wiki/Boron_nitride, Accessed November 4, 2015.

33. K.S. Kim, A. Moradian, J. Mostaghimi, and G. Soucy, "Modeling of induction plasma process for fullerene synthesis: effect of plasma gas composition and operating pressure," J. Plasma Chem. Plasma Process., vol. 30, pp. 91–110, 2010.

34. "Induction plasma technology," *Wikipedia, The Free Encyclopedia*, last modified May 8, 2014, https://en.wikipedia.org/wiki/Induction_plasma_technology, Accessed November 4, 2015.

35. Christopher Kingston, National Research Council, Montreal, Canada, private communication, October 21, 2015, http://www.nrc-cnrc.gc.ca/eng/.

36. Jérôme Pollak, Tekna Plasma Systems, Inc., Sherbrooke, Canada, private communication, October 23, 2015, http://tekna.com/.

37. Nicolas Dignard, Tekna Plasma Systems, Inc., Sherbrooke, Canada, private communication, June 18, 2015, http://tekna.com/.

38. V. Colombo, C. Deschenaux, E. Ghedini, M. Gherardi, C. Jaeggi, M. Learoux, V. Mani, and P. Sanibondi, "Fluid-dynamic characterization of a radio-frequency induction thermal plasma system for nanoparticle synthesis," Plasma Sources Sci. Tech., vol. 21, no. 4, 045010, 12 pp., 2012.

39. "Fourier transform infrared spectroscopy," *Wikipedia, The Free Encyclopedia*, last modified November 1, 2015, https://en.wikipedia.org/wiki/Fourier_transform_infrared_spectroscopy, Accessed November 4, 2015.

40. H. Chen, Y. Chen, J. Yu, and J.S. Williams, "Purification of boron nitride nanotubes," Chem. Phys. Lett., vol. 425, pp. 315–319, 2006.

41. "Boron nitride," *NIST Chemistry WebBook*, Standard Reference Database 69, http://webbook.nist.gov/cgi/cbook.cgi?ID=C10043115&Mask=80, Accessed November 4, 2015.

42. "Occupational exposure to carbon nanotubes and nanofibers," NIOSH CIB 65, Publication # 2013-145, Department of Health & Human Services, Cincinnati, OH, April 2013. http://www.cdc.gov/niosh.

43. E. Mora, T. Tokune, and A.R. Harutyunyan, "Continuous production of single-walled carbon nanotubes using a supported floating catalyst," Carbon, vol. 45, pp. 971–977, 2007.

44. A.R. Harutyunyan, "Synthesis of small diameter single-walled carbon nanotubes," Honda Motor Co. Ltd., Tokyo, Japan, US Patent # 7,981,396, July 19, 2011.

45. "Cyclonic separation," *Wikipedia, The Free Encyclopedia*, last modified October 7, 2015, https://en.wikipedia.org/wiki/Cyclonic_separation Accessed November 4, 2015.

46. J. Paiva and R.L.R. Salcedo, "Hurricane and ReCyclone systems for emission control and value added product recovery," ZKG International, vol. 64, no. 4, pp. 54–61, 2011.

47. Advanced Cyclone Systems, "Leading gas solid separation with cyclones," Product Recovery presentation, ACS Inc., Porto, Portugal, http://www.acsystems.pt/assets/misc/img/apresentacoes/ACS_PRES_RP_EN_20151216.pdf , published online December 16, 2015.

48. M. Pell, J.B. Dunson, and E.M. Knowlton "Gas-solid operations and equipment," in *Perry's Chemical Engineers' Handbook*, (D.W. Green and R.H. Perry Eds.), 8th Edition, McGraw-Hill, NY, NY, Section 17, 2008.

49. "Electrostatic precipitator," *Wikipedia, The Free Encyclopedia*, last modified October 26, 2015, https://en.wikipedia.org/wiki/Electrostatic_precipitator, Accessed November 4, 2015.

50. "Electrostatic separator," *Wikipedia, The Free Encyclopedia*, last modified May 16, 2015, https://en.wikipedia.org/wiki/Electrostatic_separator, Accessed November 4, 2015.

51. "Dust collector precipitator," *Wikipedia, The Free Encyclopedia*, last modified October 23, 2015, https://en.wikipedia.org/wiki/Dust_collector, Accessed November 4, 2015.

52. John Lenhoff, Physical Sciences Incorporated, Andover, MA, private communication, June 4, 2015, http://www.psicorp.com/.

53. Romualdo Salcedo, Advanced Cyclone Systems, Inc., Porto, Portugal, private communication, September 14, 2015, http://www.acsystems.pt/.

REPORT DOCUMENTATION PAGE

Form Approved
OMB No. 0704-0188

1. REPORT DATE *(DD-MM-YYYY)*	2. REPORT TYPE	3. DATES COVERED *(From - To)*
01-05-2016	Technical Publication	

4. TITLE AND SUBTITLE

Radio Frequency Plasma Synthesis of Boron Nitride Nanotubes (BNNTs) for Structural Applications: Part II

5a. CONTRACT NUMBER

5b. GRANT NUMBER

5c. PROGRAM ELEMENT NUMBER

6. AUTHOR(S)

Hales, Stephen J.; Alexa, Joel A.; Jensen, Brian J.

5d. PROJECT NUMBER

5e. TASK NUMBER

5f. WORK UNIT NUMBER

432938.09.01.07.92

7. PERFORMING ORGANIZATION NAME(S) AND ADDRESS(ES)

NASA Langley Research Center
Hampton, VA 23681-2199

8. PERFORMING ORGANIZATION REPORT NUMBER

L-20695

9. SPONSORING/MONITORING AGENCY NAME(S) AND ADDRESS(ES)

National Aeronautics and Space Administration
Washington, DC 20546-0001

10. SPONSOR/MONITOR'S ACRONYM(S)

NASA

11. SPONSOR/MONITOR'S REPORT NUMBER(S)

NASA/TP-2016-219194

12. DISTRIBUTION/AVAILABILITY STATEMENT

Unclassified
Subject Category 27
Availability: STI Program (757) 864-9658

13. SUPPLEMENTARY NOTES

14. ABSTRACT

Boron nitride nanotubes (BNNTs) are more thermally and chemically compatible with metal- and ceramic-matrix composites than carbon nanotubes (CNTs). The lack of an abundant supply of defect-free, high-aspect-ratio BNNTs has hindered development as reinforcing agents in structural materials. Recent activities at the National Research Council – Canada (NRC-C) and the University of California – Berkeley (UC-B) have resulted in bulk synthesis of few-walled, small diameter BNNTs. Both processes employ induction plasma technology to create boron vapor and highly reactive nitrogen species at temperatures in excess of 8000 K. Subsequent recombination under controlled cooling conditions results in the formation of BNNTs at a rate of 20 g/hr and 35 g/hr, respectively. The end product tends to consist of tangled masses of fibril-, sheet-, and cotton candy-like materials, which accumulate within the processing equipment. The radio frequency plasma spray (RFPS) facility at NASA Langley (LaRC), developed for metallic materials deposition, has been re-tooled for in-situ synthesis of BNNTs. The NRC-C and UC-B facilities comprise a 60 kW RF torch, a reactor with a stove pipe geometry, and a filtration system. In contrast, the LaRC facility has a 100 kW torch mounted atop an expansive reaction chamber coupled with a cyclone separator. The intent is to take advantage of both the extra power and the equipment configuration to simultaneously produce and gather BNNTs in a macroscopic form amenable to structural material applications.

15. SUBJECT TERMS

Boron nitride nanotubes; Plasma synthesis; Structural materials

16. SECURITY CLASSIFICATION OF:			17. LIMITATION OF ABSTRACT	18. NUMBER OF PAGES	19a. NAME OF RESPONSIBLE PERSON
a. REPORT	b. ABSTRACT	c. THIS PAGE			STI Help Desk (email: help@sti.nasa.gov)
					19b. TELEPHONE NUMBER *(Include area code)*
U	U	U	UU	51	(757) 864-9658